Biosignal-Integrated Robotic Systems with Emerging Trends in Visual Interfaces: A Systematic Review

Jaeho Lee[a,b,c,1], Sina Miri[d,1], Allison Bayro[e,1], Myunghee Kim[d,*], Heejin Jeong[e,f,*], Woon-Hong Yeo[a,b,c,g,h,*]

[a]George W. Woodruff School of Mechanical Engineering, Georgia Institute of Technology, Atlanta, GA, 30332, USA
[b]IEN Center for Wearable Intelligent Systems and Healthcare, Institute for Electronics and Nanotechnology, Georgia Institute of Technology, Atlanta, GA, 30332, USA
[c]Parker H. Petit Institute for Bioengineering and Biosciences, Georgia Institute of Technology, Atlanta, GA, 30332, USA
[d]Department of Mechanical and Industrial Engineering, The University of Illinois at Chicago, Chicago, IL, 60607, USA
[e]School of Biological and Health Systems Engineering, Ira A. Fulton Schools of Engineering, Arizona State University, Tempe, AZ, 85287, USA
[f]The Polytechnic School, Ira A. Fulton Schools of Engineering, Arizona State University, Mesa, AZ, 85212, USA
[g]Wallace H. Coulter Department of Biomedical Engineering, Georgia Institute of Technology and Emory University School of Medicine, Atlanta, GA, 30332, USA
[h]Institute for Materials and Institute for Robotics and Intelligent Machines, Georgia Institute of Technology, Atlanta, GA, 30332, USA
[1]These authors contributed equally.
*Correspondence author email: whyeo@gatech.edu (W.Y.); heejin.jeong@asu.edu (H.J.); myheekim@uic.edu (M.K.)

Abstract
Human-machine interfaces (HMI) are currently a trendy and rapidly expanding area of research. Interestingly, the human user does not readily observe the interface between humans and machines. Instead, interactions between the machine and electrical signals from the user's body are obscured by complex control algorithms. The result is effectively a one-way street, wherein data is only transmitted from human to machine. Thus, a gap remains in the literature: how can information be effectively conveyed to the user to enable mutual understanding between humans and machines? Here, this paper reviews recent advancements in biosignal-integrated wearable robotics, with a particular emphasis on "visualization" – the presentation of relevant data, statistics, and visual feedback to the user. This review article covers various signals of interest, such as electroencephalograms and electromyograms, and explores novel sensor architectures and key materials. Recent developments in wearable robotics are examined from control and mechanical design perspectives. Additionally, we discuss current visualization methods and outline the field's future direction. While much of the HMI field focuses on biomedical and healthcare applications, such as rehabilitation of spinal cord injury and stroke patients, this paper also covers less common applications in manufacturing, defense, and other domains.

1. Introduction

HMI occupies a prominent place within the interdisciplinary research landscape, bridging intricate human biological processes with cutting-edge technological advancements [1]. Over the years, this domain has experienced significant growth, largely driven by transformative innovations in soft sensors and wearable robotics [2], [3], [4], [5]. These advancements enable the precise conversion of human physiological signals into formats that machines can readily interpret and act upon [6], [7]. However, within the expanding corpus of HMI literature, the integration of visual interfaces remains inadequately addressed. This gap not only underscores the uniqueness of this manuscript but also emphasizes the urgent need for exploration in the HMI research field. As HMIs become more commonplace across various sectors, this work aims to encourage further research and provide a clearer perspective on the integrated role of sensors, robotics and visual interfaces in HMIs. The scope of this paper is threefold: First, we delve into the field of soft sensors. These tools epitomize the interface of human intent and machine functionality, with their effectiveness largely contingent on the accurate interpretation of biological signals [8], [9], [10], [11], [12], [13]. Alongside this, we highlight the latest developments in sensor architectures and materials, emphasizing their crucial role in improving the responsiveness and accuracy of these devices [3], [14]. Our attention then shifts to the foundations of robotics, investigating applications, control strategies and mechanical aspects. This approach highlights the importance of a harmonious relationship between the software directives and the hardware components, ensuring overall efficiency and reliability in HMIs [15], [16], [17]. Finally, we turn our attention to the often-overlooked aspect of visualization. As the demand for more transparent human-machine interactions grows, visualization becomes increasingly vital, offering ways to present complex machine feedback in a user-friendly manner [18], [19], [20], [21]. Collectively, these sections converge on a singular goal: to transform HMI from a one-way interaction into a two-way conversation where both humans and machines can understand and respond to each other. Through this comprehensive review, we provide an in-depth look into the current landscape and potential future of HMI. For a consolidated understanding of the interconnected roles of sensors, robotics, and visual interfaces, Fig. 1 presents an overview of the integration and interdependence of these systems.

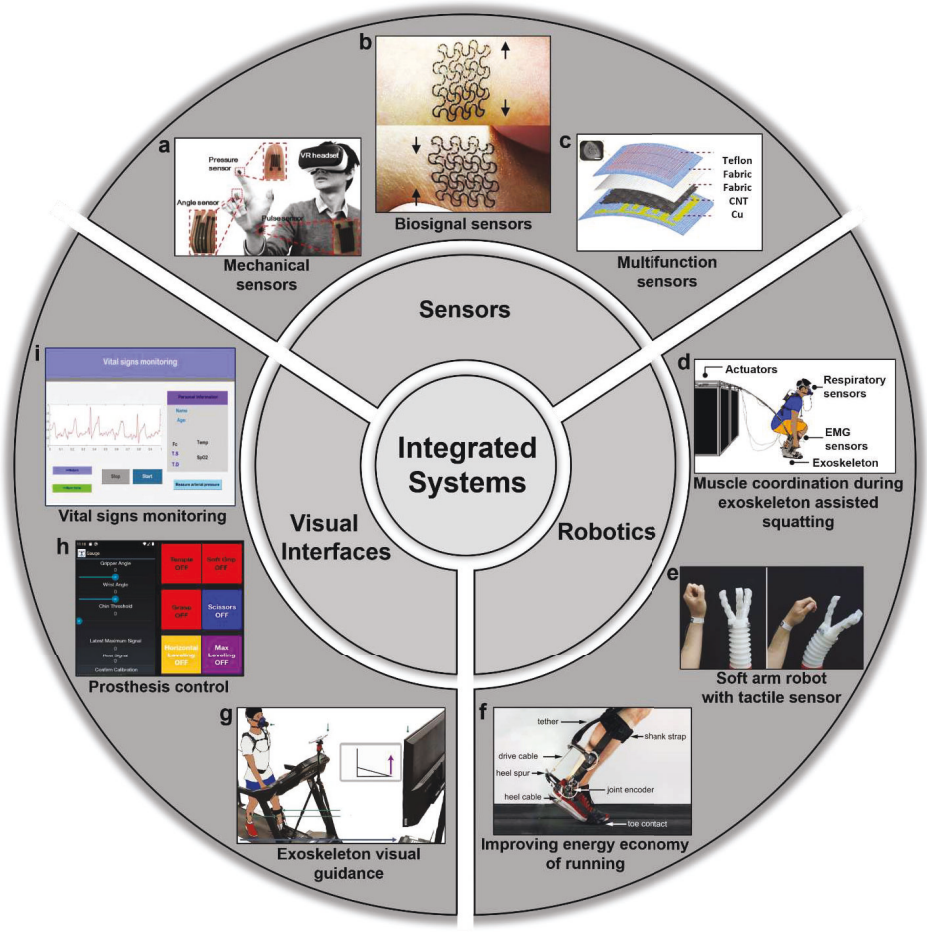

Figure 1. Elements of biosignal-integrated robotic systems. (a) Several strain sensors used to measure joint angles, fingertip pressure, and pulse. Reproduced with permission [22]. Copyright 2018, Elsevier. **(b)** Stretchable EMG electrodes collect muscle activity data for multimodal human-machine interfaces. Reproduced according to the terms of the CC BY license [23]. Copyright 2020, the authors, published by Springer Nature. **(c)** Design of a textile-based sensor capable of detecting biosignals (e.g., pulse rate) as well as mechanical signals (e.g., joint dynamics). Reproduced with permission [14]. Copyright 2022, Elsevier. **(d)** Studying muscle coordination and recruitment through synergy analysis during use of a robotic ankle-foot exoskeleton. Reproduced according to the terms of the CC BY license [24]. Copyright 2023, the authors, published by Springer Nature. **(e)** Control of a soft arm robot manipulator with tactile sensors. Reproduced according to the terms of the CC BY license [14]. Copyright 2022, Elsevier. **(f)** An ankle exoskeleton evaluated for reduction of metabolic cost. Reproduced with permission [25]. Copyright 2018, AAAS. **(g)** A visual guidance screen can streamline training sessions for

new users of exoskeletons. Reproduced according to the terms of the CC BY license [18]. Copyright 2022, the authors, published by Springer Nature. **(h)** Example of a mobile application that can both monitor and control usage of an arm prosthesis. Reproduced according to the terms of the CC BY license [26]. Copyright 2022, Springer Nature. **(i)** User interface for a nursing robot displaying real-time signals, including heart rate, temperature, and blood oxygen**.** Reproduced with permission [21]. Copyright 2023, Springer Nature.

Robotic systems have experienced significant evolution, mirrored in the progression of control block diagrams [27]. These diagrams visually depict control systems, elucidating the interactions between a robot's feedback loops and components [28]. The evolution of robotic systems using this block diagram approach is presented in Fig. 2. We use the term "intelligent robotics" in this figure about recent robotic systems with a high degree of integration, cooperation, and communication with other elements of an increasingly complex control system. Additionally, we believe the capability to respond to new and emerging stimuli, especially physiological signals, to be an important characteristic separating newer robots from previous generations. Historically, robotic systems relied primarily on mechanical signals and non-physiological methods, with interactions limited to physical connections between robot links and human limbs. By the early 21st century, physiological sensors such as electrocardiography (ECG) and electromyography (EMG) sensors, initially designed to study human physiology [29], [30], were incorporated into robotics, paving the way for biofeedback control. This focus constrained the depth of understanding regarding human responses and intentions [31]. The "human in the loop" or "body in the loop" concept, combined with these sensors, marked an important shift in robot control considering unknown human-robot interactions. This perspective regarded both the robot and the human as integral parts of a cohesive control system [31], [32], [33]. Through this perspective, controllers could design strategies attuned not only to the robot's functionalities but also to human states and intentions [34], [35]. Recent trends have centered on forging an even stronger synergy between humans and robots [36]. Advances in visualization, including extended reality, promise to redefine this dynamic [18], [19], [20], [21]. One of its primary objectives is a harmonious co-adaptation between the two entities.

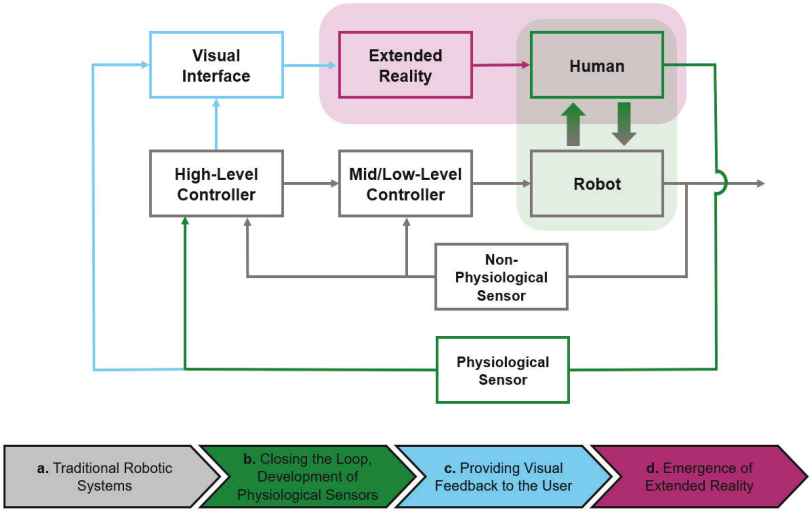

Figure 2. Evolution of intelligent robotics systems. (a) Block diagram representation of the conventional robotic control system reliant on non-physiological signals for robot control, with human-robot interaction occurring solely through mechanical interactions between robot and human body. **(b)** Closing the loop of by looking at the human and robot as an interactive system. Achieved through capture of human physiological data using bio-sensors, enabling the controller to harmonize robot behavior with the human condition. **(c)** Introduction of visual feedback to enhance user comprehension of controller actions and human status, facilitating user adaptation to the system. **(d)** The advent of novel visualization methods, such as virtual and augmented reality, driving enhanced interaction between human and robotic systems.

We followed the Preferred Reporting Items for Systematic Reviews and Meta-Analyses (PRISMA) process for literature retrieval and selection [37]. To capture the most recent developments in the field, we conducted a focused review spanning five years from 2018 to 2023. Our initial search in the SCOPUS database, using keywords ("interface" OR "visual") AND ("sensor" OR "signal" OR "feedback" OR "biosignal" OR "biofeedback" OR "physiological signal") AND ("robot" OR "exoskeleton" OR "prostheses" OR "exosuit" OR "orthoses"), yielded 784 records, supplemented by an additional 19 records from other sources. The first screening phase entailed the exclusion of records based on a set criterion: plant and animal research, inaccessible texts, duplicate studies, incomplete studies, and papers not available in English. This resulted in the exclusion of 209 records. Subsequently, in the second phase, we reviewed titles and abstracts, eliminating 381 records that did not directly relate to biosignal-integrated robotics systems with visual interfaces. The final screening phase involved a comprehensive review of the full texts. Here, 112 records were further excluded for not aligning specifically with the theme. In other words, the texts did not include soft sensors, wearable robotics, and/or visual interfaces. Following this three-tiered screening process, we identified a corpus of 101 papers, which form the basis of our review. Fig. 3 provides a visual overview of the PRISMA process undertaken in this work.

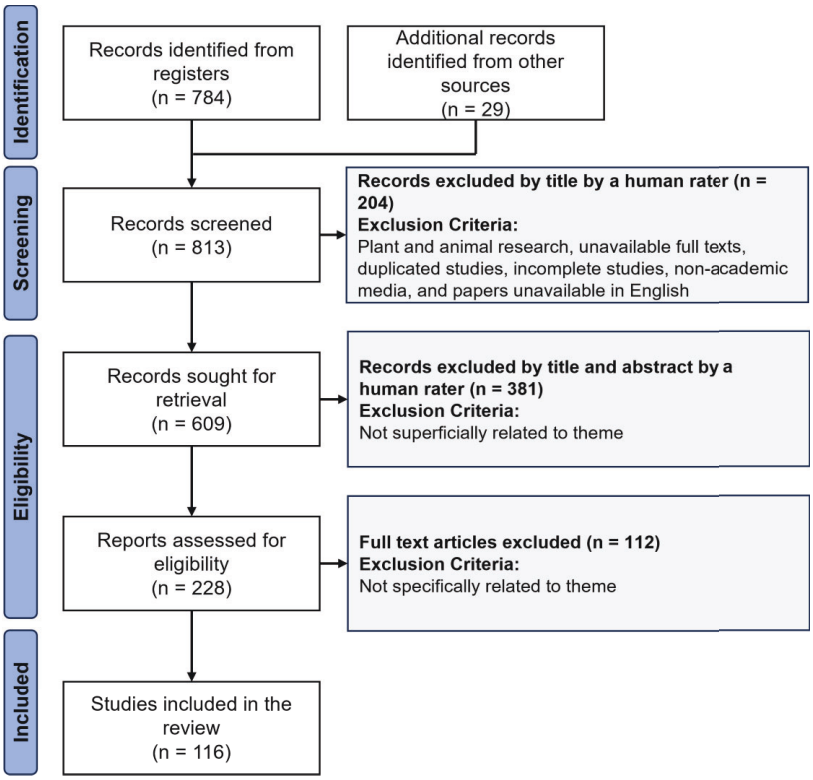

Figure 3. Systematic review process. Selection process flowchart of the included studies for this systematic review, following the PRISMA protocol.

2. Sensors

Sensors serve as the fundamental link between human users and robotic systems. An increasing number of users are engaging with their robots by utilizing various biosignals, which are natural electrical potentials generated by the human body, ranging from the heart and brain to skeletal muscles and other organs. Some sensors also capture physiological phenomena that do not inherently generate electrical potentials, such as the dynamic movements of joints, and convert them into usable electrical signals. Harnessing the information streams within the human body, sensors play a critical role in shaping HMI. Recent developments in sensor technology aim to enhance key performance metrics such as signal-to-noise ratio, sensitivity, and packaging. Additionally, wearable sensors designed for integration with robotics explore additional dimensions, including environmental sustainability, biocompatibility, and optimizing user comfort [38], [39]. In this section, we will showcase recent advancements in sensor design, materials, and manufacturing techniques across various sensor classes commonly integrated into robotic systems and visual interfaces.

2.1 EEG sensors

One of the most widely used biosignals is electroencephalography (EEG), a noninvasive process that involves the use of scalp electrodes to detect surface-level electrical currents originating from brain activity, specifically cortical neurons. These signals are primarily generated by flow of ions such as Na+ and K+ through neuron membranes. However, measuring potentials from surface electrodes encounters challenges related to signal degradation as they pass through multiple layers of skin and bone. EEG signal amplitudes typically display very small values, spanning from 0.5 to 100 μv. To address this, various amplification devices are introduced into the signal chain, serving to reject noise, eliminate interference from other body potentials, and apply gain. Both analog and digital filtering techniques are employed to separate distinct EEG signal frequencies [40]. EEG signals are commonly categorized into several recognized ranges: delta waves ($\boldsymbol{\delta}$, 0.1-4 Hz) associated with deep sleep and unconsciousness, theta waves ($\boldsymbol{\theta}$, 4-8 Hz) commonly linked with rapid eye movement, alpha waves ($\boldsymbol{\alpha}$, 8-13 Hz) corresponding to relaxed mental state, and beta ($\boldsymbol{\beta}$, 13-30 Hz) or gamma ($\boldsymbol{\gamma}$, 30-70 Hz) waves connected to focus, alertness, and higher motor function [41]. This data serves multiple purposes, primarily offering valuable clinical insights to physicians. For example, EEG is a critical component of polysomnography exams for assessing sleep disorders and serves as the gold standard for diagnosing epilepsy [40]. However, of particular interest in this context is EEG's essential role in establishing connections between humans and robotic systems through classifiable signal patterns [42]. In particular, evoked potentials (EP) and event-related potentials (ERP) involve distinctive patterns that emerge in an electroencephalogram as subjects react to specific external stimuli or mental cues, often appearing as intermittent and low-amplitude signals [40]. Visual interfaces are now being integrated with sensing and robotics systems to provide stimuli for EP/ERP classification and control experiments. Once these signals are clearly identified, they become powerful tools that can be incorporated into robotic control systems and extended reality platforms [43]. This approach is especially popular in rehabilitation robotics, where motor imagery, linked with EEG, can actuate assistive devices [2], [44], [45], [46], [47], [48]. Traditional clinical EEG setup employs a large array of wired electrodes evenly distributed across the patient's scalp. Conductive gel is often applied beneath each electrode to reduce skin impedance. Electrode placement usually follows the 10-20 system, an internationally standardized guideline for arranging up to 21 electrodes [49]. Common drawbacks include bulkiness, limited portability, extensive user preparation, and skin irritation caused by the conductive gel. The limitations of complex wired systems become particularly evident when testing robotics applications, where users are generally more physically active compared to clinical EEG studies.

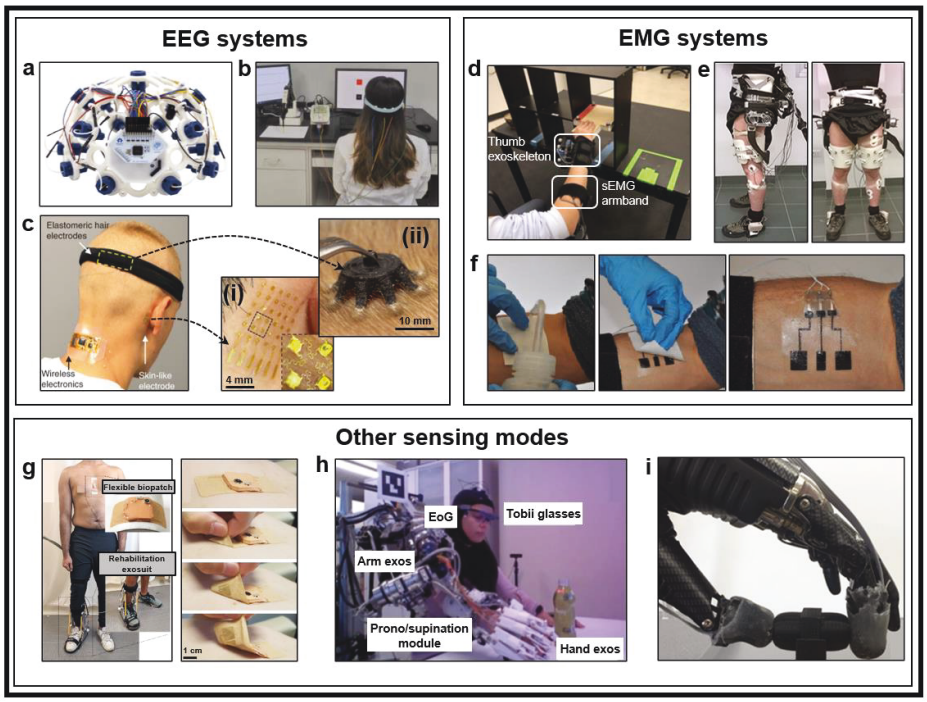

Figure 4. Examples of recently developed sensor systems, highlighting commonly used physiological signals. (a) Modular EEG cap in 16-channel configuration used for digital hemiplegia rehabilitation. Reproduced according to the terms of the CC BY license [50]. Copyright 2022, IOP. **(b)** 3-channel EEG headband with custom FLG/TiO_2 electrodes interfacing between a user and a robotic arm. Reproduced with permission [9]. Copyright 2023, Elsevier. **(c)** An EEG-based universal brain-machine interface featuring (i) aerosol jet printed skin-like electrodes and (ii) flexible dry hair electrodes. Reproduced with permission [51]. Copyright 2019, the authors, Springer Nature. **(d)** An EMG armband provides muscle activation data to guide a thumb exoskeleton. Reproduced according to the terms of the CC BY license [52]. Copyright 2018, MDPI. **(e)** Surface EMG electrodes used for control of a hip exoskeleton. Reproduced according to the terms of the CC BY license [53]. Copyright 2018, Frontiers Media SA. **(f)** Tattoo-inspired printed circuits for monitoring EMG and other biosignals. Reproduced with permission [54]. Copyright 2018, American Chemical Society. **(g)** Wearable ECG monitor for control of an ankle-foot orthotic. Reproduced according to the terms of the CC BY license [12]. Copyright 2023, the authors, Springer Nature. **(h)** EOG interface and eye-tracking glasses used in support of an arm exoskeleton. Reproduced according to the terms of the CC BY license [55]. Copyright 2019, MDPI. **(i)** Tactile fingertip sensor for prosthetics. Reproduced with permission [56]. Copyright 2018, AAAS.

Still, some researchers opt to use commercial clinical EEG equipment due to convenience or familiarity. Various commercial EEG systems have been effectively integrated with robotics and visual interfaces. For example, OpenBCI offers a modular EEG kit that has served as a platform

for rehabilitating digital hemiplegia patients and operating smart home appliances (Fig. 4a) [47], [50]. This example represents many rigid commercial EEG devices, highlighting their limitations in comfort and portability. In another study, Baka et. al. used a 34-lead cap by Compumedics Neuroscan to study emotional states during human-robot interactions, showing the 10-20 system's capacity for expansion to achieve finer resolution [57]. However, the commercial systems like Neuroscan and others used for general EEG data collection tend to be relatively cumbersome, whether rigid or flexible in design [58], [59], [60], [61]. Although smaller, more flexible, and wireless devices tailored for specific HMI applications have the potential to address these limitations, they are not yet widely available commercially. Recent advances in EEG technology have been addressing the aforementioned common issues. In addition, new devices are being designed as dedicated companions to particular robotic systems, allowing for improved comfort through optimized form factor and placement. To tackle electrode impedance and concerns related to conductive gel, Li et. al. developed a novel dry EEG electrode incorporating few-layer graphene (FLG) nanosheets and titanium oxide (TiO_2) nanotubes (Fig. 4b) [9]. The custom electrode involved potentiostatic anodization for the TiO_2 nanotube arrays and plasma jet chemical vapor deposition (CVD) for the FLG sheets (Fig. 4c). The length of the nanotubes could be controlled by adjusting the anodization time, preserving the proper three-dimensional cross-wrapping of the FLG nanosheets. This innovative design offers several advantages over a traditional Ag/AgCl or gel electrode. First, by using a semiconductor material like graphene instead of metal, the electrode functions in a capacitor or "non-contact" mode, measuring ion current and converting it to electrical current, rather than directly measuring electrical current. This approach typically reduces noise while potentially decreasing signal amplitude. However, the incorporation of TiO_2 nanotubes creates an exceptionally favorable environment for electron transport through nanopore channels, mitigating amplitude loss and resulting in a higher overall signal-to-noise ratio (SNR). Additionally, the FLG/TiO_2 electrode uses sweat absorbed from the skin surface for ion conduction, eliminating the need for applying, maintaining, and cleaning conductive gel. Finally, the device is customized for a specific application: teleoperation of a robotic arm. This specification allows the device to target only the three occipital positions (O1, Oz, O2) of the standard 10-20 system to complete the control task. By eliminating the other electrode positions, the entire system can be downsized into a headband, significantly improving long-term comfort. Li et. al. demonstrated high amplitude (8.6 μV, nearly double that of their Ag/AgCl control) and SNR (as high as 76.8 dB, exceeding that of the Ag/AgCl control) during EEG measurement using a FLG/TiO_2 electrode with a one-hour TiO_2 deposition time. These electrodes exhibited stable SNR, signal correlation coefficient with Ag/AgCl control, and scalp resistance during two hours of continuous use, as well as 30 minutes of daily use over one month. Furthermore, the EEG headband was successfully used to measure steady-state visually evoked potentials (SSVEP) at multiple frequencies, which were then implemented to command a robotic arm to write letters. This study demonstrates the potential of unique 1D and 2D nanomaterials as solutions to current challenges in biosignal sensor performance. Wang et. al. have developed a compact, portable EEG system designed for integration with VR headsets and various robots through teleoperation. Their wearable device resembles earbuds and features two custom dry electrodes and microscale Bluetooth modules [62]. The electrode design eliminates the need for skin preparation and allows for concurrent electrooculogram (EOG) recording (see Sections 2.3 and 2.5 respectively for further discussion of EOG and multimodal sensing). Employing independent component analysis and support vector machine (SVM) techniques, the EEG system achieves a remarkable 95% accuracy in interpreting brain signals associated with eye movements and facial expressions. Studies using this device have successfully implemented human facial expressions to control teleoperated drones, showcasing its potential for unobtrusive sensor integration with VR devices and robotics. Finally, Mahmood et. al. have introduced a flexible, wireless EEG system paired with a convolutional neural network for SSVEP classification [51]. This device tackles the limitations of traditional EEG setups, such as their obtrusive form factor

and inconvenient wiring, by employing skin-conformal packaging and wireless data transmission. Similar to the design by Li et. al., this wearable scalp electronics system optimizes electrode placement for HMI applications. Dry, elastomeric electrodes with flexible legs cover the O1, Oz, and O2 positions, adapting to the hairy skin of the scalp (Fig. 4c, inset ii). As the headband is placed over these electrodes, the legs splay to push aside hair and achieve maximum contact area. An aerosol-jet printed stretchable silver electrode serves as a ground applied at the mastoid (Fig. 4c, inset i). Finally, the data acquisition and processing unit consists of a flexible printed circuit board encapsulated in a soft elastomer, attached to the back of the user's neck. Mechanical testing confirmed reliable wireless transmission of EEG data under 180° bending. Additionally, cyclic bending, compression, and stretching tests show minimal (<10%) resistance change for the interconnects, electrodes, and circuit board. Signal quality and classification accuracy were compared against two commercial devices: a 32-channel gel electrode EEG system and 8-channel clip-on wireless system with dry electrodes. The newly developed EEG device easily outperforms the two commercial options in capturing 12.5 Hz SSVEP signals, offering an average SNR of 46.6±2.16 dB compared to 16.94±4.60 dB (conventional gel electrode system) and 28.89±2.28 dB (wireless system). Both offline and real-time EEG classification using SVM and convolutional neural network (CNN) models display high accuracy, achieving values of 94.54±0.90% and 94.01±3.6% respectively. An information transfer rate (ITR) of 122.1±3.53 bits per minute is competitive with commercial options. Practical applications include real-time wireless control of an electric wheelchair, a small vehicle, and presentation software, with data and results visualized through a custom Android mobile app. This system represents a substantial improvement in user comfort, portability, and packaging optimization, along with enhancements in key performance metrics such as SNR, indicating progress towards a more field-ready, universal HMI platform.

2.2 EMG sensors

2.2.1 Background

EMG is another biosignal related to naturally occurring electrical activity in the human body. Rather than monitoring the brain directly, EMG focuses on the potentials generated in skeletal muscles by the peripheral nerves. As motor neurons activate their associated muscle fiber bundles, electrodes can be used to detect the voltage changes during contraction and relaxation. An increase in voltage is linked to firing of action potentials during muscle contraction, while potential drops are associated with repolarization. There are two forms of electrode used during EMG measurements. Intramuscular electrodes consisting of needle or fine wire can be inserted under the subcutaneous layer directly into the muscle of interest to measure potentials. By contrast, surface electrodes are attached to the skin and do not interface directly with the muscle tissue. Both methods offer certain advantages and disadvantages. Surface EMG (sEMG) is noninvasive and simpler to implement but suffers in terms of high-resolution targeting of specific areas. Intramuscular measurements are invasive, and hence not as suited to HMI applications. However, they generally yield more accurate data on individual muscle fibers [63]. Much like EEG, raw EMG signals are low amplitude (around -5 to 5 mV) and often drowned out by ambient noise or motion artifacts. In addition, EMG signals often display crosstalk from muscle fibers adjacent to the target area. This is of particular concern for HMI applications, as sEMG is the preferred method and tends to suffer from crosstalk to a greater degree. Various high/low-pass and notch filters are used to remove noise or motion artifacts. Furthermore, advances in sensor design are improving skin conformality to further eliminate noise. Wavelet analysis is often implemented to decompose raw EMG data into constituent potentials from individual motor units. Other popular signal processing techniques include autoregressive models, other time-frequency approaches such as Wigner-Ville distribution, and artificial neural networks [63] Because of widespread interest in active exoskeletons, prostheses [64], and orthoses, EMG has emerged as a popular option for biosignal integration into robotic control algorithms and visual interfaces. By segmenting

a user's EMG signal into specific muscle activation phases, a sequence of their movements can be recreated. With adequate data transfer rates, this information can be incorporated into real-time control algorithms. Many studies use commercial EMG acquisition units such as those offered by Delsys and Ottobock [15], [65], [66], [67], [68], [69], [70], [71], [72], [73]. These have been leveraged into biosignal-controlled upper and lower body robotics (Fig. 4d and 4e) as well as the Lokomat rehabilitation system [53], [74], [75], [76], [77], [78], [79], [80], [81]. Both real-time and offline EMG signal processing and muscle activity classification are used. While these studies provide insightful results with clinical significance, their practical applications are limited by the lack of portability. Commercial EMG acquisition systems are often centered around large, cumbersome processing units that are wired for power and peripheral devices.

2.2.2 Improving comfort and portability

For successful adoption and field use in roles such as industrial work or support with activities of daily living, the bulky, static nature of existing systems is a hindrance. Especially concerning is the lack of low-profile sensing options and wireless data transfer capability. Minimizing form factor and breaking free from wired systems will be critical requirements for many practical use cases. Several studies have addressed these issues by presenting ultrathin, skin conformal, wireless EMG acquisition devices. For example, Dong et. al. developed a stretchable sEMG electrode based on a second-order self-similar serpentine pattern [82]. The slim, lightweight design was created with wireless use in mind, ensuring portability and user comfort. The electrodes are fabricated on a silicon carrier wafer by sputtering 0.3 μm-thick gold between spin-coated polyimide (PI) layers. Oxygen reactive ion etching is employed to pattern the electrode before the top layer of PI is applied. Photoresist process parameters were tuned to obtain 50 μm line width. The electrode displays excellent skin conformality and compliance under large deformation. Finite element analysis and optical imaging concur that the electrode easily sustains 40% strain, meeting the requirement to stretch with human skin (up to 30% strain). Using ZigBee transmitting nodes and a DAQ, the electrodes successfully transfer EMG data from the user to a wheeled robot in real time. A variety of bodily motions, such as wrist flexion and finger bending, are demonstrated to drive the mobile robot with full range of motion. This system is an example of how thin, flexible materials and unique micro- and nano-scale architectures can improve the EMG data acquisition process for HMI applications.

2.2.3 Fabrication methods and materials

Many research teams are using new manufacturing techniques and materials to tackle the problems facing the wearable EMG design space. Lopes et. al. present a novel hydroprinted electronic skin (e-skin) incorporating the unique properties of eutectic gallium-indium (EGaIn), a liquid metal alloy [54]. The e-skin is ultrathin (~5 μm) and stretchable, in addition to having excellent skin conformality due to the hydrographic transfer process. Various shapes can be created to build a complete sensor circuit featuring electrodes and interconnects with microscale line width and pitch. Electronic and mechanical stability is excellent, surviving applied strains of over 70% with no breakage and minimal resistance change. The fabrication methods are of particular interest because they not only permit for these desirable qualities but also eliminate expensive and time-consuming cleanroom processes. To achieve reliable hydrographic transfer onto 3D surfaces, the process begins with printing the circuit onto tattoo transfer paper (TTP) with a standard office laserjet printer. Silver epoxy is spread over the TTP and selectively adheres to the laserjet toner when cured, allowing subsequent application of liquid EGaIn. Using a HCl vapor or 2wt% acetic acid solution, the EGaIn selectively wets to silver, creating a complete circuit with high conductivity. The entire process can be completed at low temperature with off-the-shelf office equipment, a great achievement for high-throughput manufacturing of ultrathin wearable sensors. The e-skin can be transferred to the human body through a variety of water-based methods. When using TTP, the device can be directly applied to the biosignal acquisition area and wetted before

peeling the backing layer (Fig. 4f). With hydrographic paper, the entire printed device is suspended on top of a water bath while the target object is passed through it vertically. When the target breaks the surface of the bath, the e-skin sticks and conforms to its shape. These unique transfer techniques enable superior adhesion and conformality to the shapes of the human body, decreasing motion artifact noise and improving user comfort. HMI applications are further supported by the e-skin's ability to interface with surface mount electronic (SMD) components through a thin film of Ag-coated Ni particles mixed into polyvinyl alcohol (PVA). By evaporating water from the PVA film while the device is held in a magnetic field, the Ni particles vertically align to form conductive vias between the printed circuit and any components placed over it. This technique also allows the e-skin to connect to other circuits, expanding options for HMI peripherals. The system's versatility is demonstrated by connecting a flexible printed circuit board (fPCB) EMG acquisition unit to the e-skin and applying it to a subject's forearm. The EMG signal is used to control a hand prosthetic which itself features an e-skin circuit with integrated LEDs and touch pads providing visual feedback and additional command options, respectively. Kwon & Kim et. al. used other printing methods to fabricate a comprehensive flexible, wireless EMG system consisting of a data acquisition fPCB and electrodes [23]. The device is compact and lightweight, improving overall comfort in multi-channel use for detection of detailed muscle patterns. Another benefit of this system is that printing avoids the complex and costly cleanroom fabrication processes of traditional electronics manufacturing. Aerosol-jet printing is deployed to print functionalized conductive graphene (FCG) electrodes, Ag traces/pads, and PI insulating and structural layers. Due to the unique properties of FCG as an oxidation barrier, SMD components for data processing and Bluetooth connectivity can be soldered directly to FCG-coated Ag pads. The entire device weighs less than 5 g and measures under 2 mm in height. The mechanical performance of the FCG electrodes and fPCB are both excellent. Electrodes displayed resilience to cyclic 180° bending (100 cycles, 1.5 mm radius) and up to 60% stretching. The circuit showed negligible resistance shift and deviation in EMG signal strength over similar cyclic bending conditions. Signal quality was evaluated against the gold standard gel electrodes as well as commonly used Ag and Au electrodes. The improved skin conformality of the FCG electrodes led to SNR on par with gel electrodes and greater than that of both Ag and Au electrodes. All of these demonstrated characteristics lend themselves to smooth integration with robotics and visual interfaces in HMI applications. In this study, three devices were used to target the brachioradialis, palmaris longus, and flexor carpi ulnaris muscles in the forearm. Full control of all five digits was demonstrated through real-time wireless teleoperation of a custom robotic hand with 98.6% classification accuracy, a task that would require over triple the channels using a traditional EMG acquisition system. Even a single sensing unit is sufficient for many control tasks. Here, a single EMG device is used to remotely fly a quadcopter drone and drive a wheeled vehicle, as well as cycle through a slide deck with signal processing via CNN showing classification accuracy of 99%. The devices were also integrated with Bluetooth to an Android tablet displaying real-time EMG data plotting. Overall, devices presented in the studies discussed here represent a recent trend towards flexible, low-profile epidermal electronics for EMG acquisition. Novel fabrication techniques and materials feature at the forefront of this shift, showing their benefits in practical HMI applications.

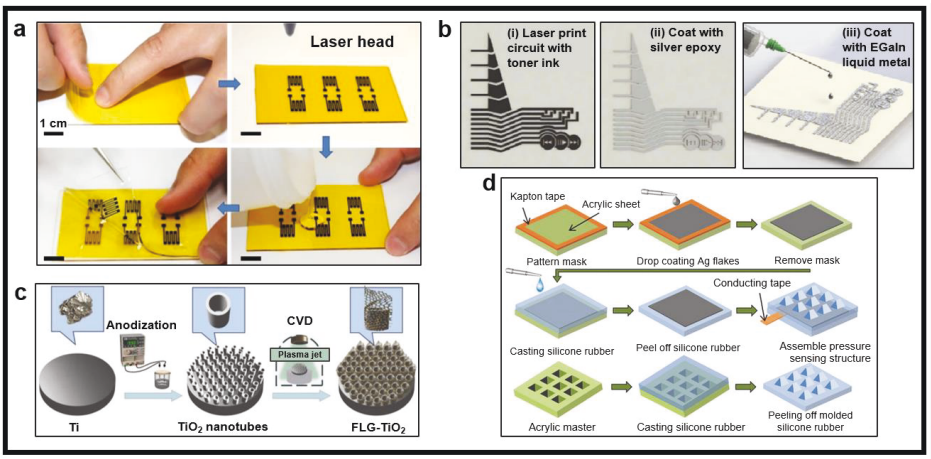

Figure 5. Selection of fabrication processes for sensors in integrated systems. (a) Patterning and transferring laser-induced graphite for use in stretchable strain sensors. Reproduced with permission [22]. Copyright 2018, Elsevier. **(b)** Hydroprinting method for rapid, low-cost fabrication of flexible circuits and sensors. Reproduced with permission [54]. Copyright 2018, American Chemical Society. **(c)** Process for fabrication of EEG electrodes using few-layer graphene and TiO_2 nanotube arrays. Reproduced with permission [9]. Copyright 2023, Elsevier. **(d)** Molding three-dimensional structures for triboelectric sensing skins from silicone rubber and silver flake. Reproduced with permission [83]. Copyright 2018, John Wiley and Sons.

2.3 Other bioelectric sensors

Here, we will explore less commonly used electrical signals generated by the human body. Recent work has revealed compelling examples of integrated robotic systems using sensors for ECG, EOG, and other biosignals. ECG is a biosignal that targets the depolarization and repolarization of cardiac muscle as the heart is stimulated by the sinoatrial node. The natural coupling of specialized conductive tissues with mechanical pumping provides unique insight into the cardiac rhythm [84]. Traditionally measured in clinical settings to diagnose cardiac disorders such as arrhythmias or ischemia [84], there has been a recent study integrating ECG as a control input for a robotic system. Kim et. al. present a soft wearable ECG patch that provides estimation of metabolic cost (see Section 2.4) to optimize power delivery of an ankle-foot orthotic (AFO) during squatting, walking, and running [12]. The ECG device consists of three 210 nm-thick gold electrodes paired to a data acquisition fPCB by serpentine interconnects, all mounted on a stretchable, breathable medical tape substrate and encapsulated in soft silicone elastomer. The compact, flexible design allows for robust mechanical performance up to 50% elongation. Electrical resistance change of the electrodes and interconnects is less than 1% over hundreds of cycles at 30% strain. Heart rate variability root mean square of successive differences (HRV-RMSSD) is calculated from the ECG signal and correlated to metabolic cost with a strong Pearson R of -0.758 and SNR of over 25 dB. This is a major improvement in terms of real-time signal quality, user comfort, and portability over traditional methods of measuring metabolic cost, which require bulky masks, tubing, and peripheral processing equipment. The ECG-based exoskeleton feedback method presented shows promise for future adoption of biosignal-integrated robotics and visual interfaces in labor-intensive work environments. EOG refers to measurement of the potential difference within the eye. By placing electrodes around the eye, the eye motion can be deciphered from rotation of the dipole formed by the cornea (front side) and retina (back side)

[85]. It can achieve high rates of classification accuracy in HMI applications, but it is susceptible to noise and there is limited room for multiple functions [86]. Tan et al. utilized EOG control as part of a rehabilitation robot system with integrated visual interface [87]. The EOG signal is used situationally during training exercises with a robotic arm to navigate menus in the integrated display screen. Ban et al. developed a 3D-printed wireless EOG headband with gold electrodes that performed competitively with commercial options in SNR and impedance. A proof of concept HMI application was implemented through remote control of a robotic wheeled vehicle [88]. Crea et al. also incorporated EOG into actual robotic control, demonstrating successful manipulation of a wheelchair and arm exoskeleton system [89]. Badesa et al. expanded upon this, using EOG and eye tracking data to guide an arm exoskeleton through object reach-and-grasp tasks [55]. Specifically, a right horizontal oculoversion triggered the exoskeleton to reach for an object in front of the user, a movement with 99.85% success rate. Interestingly, the EOG-based control scheme was found to cause reduced stress response and mental load compared to an EEG-based algorithm driving the grasping portion of the training task. One more set of signals to note are galvanic skin response (GSR) and photoplethysmogram (PPG). GSR, also known as electrodermal activity (EDA) and several other names historically, is a measure of the conductance of the epidermis. Physiologically, this is linked to the activation of sweat glands during autonomic nervous system response [90]. Meanwhile, PPG tracks the change in blood volume of microvasculature. This is often achieved by placing a light source on the skin and using a photodetector to measure shifts in light intensity from the varying perfusion levels of the vascular bed. This signal can be used to calculate a wide variety of cardiac features such as blood oxygen and heart rate, which are also physiologically linked to autonomic nervous function [91]. Although PPG is not strictly a naturally occurring electrical signal like GSR, it is introduced in this section due to its use in combination with PPG for integrated robotics and visualization systems. More specifically, the heavy overlap of the physiological underpinnings of both signals is highly relevant in monitoring stress response and mental state [90], [91], [92]. Multiple studies have utilized GSR and PPG sensors in tandem to characterize how users emotionally interact with social robots in an effort to inform robot designs of the future [93], [94], [95], [96]. Although this review has thus far tended to focus on wearable robotics, systems such as the nursing robot developed by Uluer et. al. for hearing impaired children must also be considered relevant to the topic [19]. The robot presented here displays real-time response to user GSR/PPG signals and features a highly interactive visual interface to administer audiometry tests.

2.4 Non-bioelectric sensors

Not all sensors depend purely on the natural electrical potentials of the human body (Fig. 4g-i). Mechanical sensors are also commonly used in human interactions with robotic systems, translating physical motions of the body into electrical signals for processing. A diverse selection of movements can be detected and applied towards integrated robotics and visual interfaces. One popular sensing target is joint kinematics such as force, torque, and angle. These signals are used for a variety of robotic form factors and are particularly applicable to impedance control [97]. Rotary encoders and inertial measurement units (IMUs) are both popular in traditional rigid wearable robotics for gathering quantities such as joint angles [98], [99]. However, as robots themselves evolve toward flexible designs, sensors must follow suit. New soft sensor designs and data processing methods are helping researchers to do more with less, gathering kinematic data with fewer, more user-friendly sensors [100]. Sun et. al. worked with force/torque sensors in an upper body exoskeleton, developing a Kalman filter-based approach for reducing sensor channels to improve wearability and joint alignment. The study was able to show that fusion of data from just two force/torque sensors (arm, wrist) matched the performance of the full complement (two arm, one wrist) in terms of operator-exoskeleton power exchange and actuation stress [101]. A more niche sensing option is mechanomyography (MMG). As the mechanical counterpart to EMG, MMG recognizes muscle activation sequences, but does so by detecting dimensional

changes and lateral movement of the muscle from the surface. These signals can be gathered with a variety of mechanical sensors, including piezoelectric devices and microphone chips [102]. Wilson et. al. combined six MEMS microphone MMG sensors and two IMU sensors to create a custom teleoperation armband with accompanying control algorithm. The system was first successfully integrated with the Oculus Rift virtual reality goggles as a controller, then used to remotely operate a robotic arm [103]. Another major target is pressure sensing for the implementation of tactile feedback in prosthetics. Accurate and consistent pressure data is critical for the successful application of any feedback model, thus leading researchers to explore new sensor designs to fulfill this need [104]. Existing wearable pressure sensors, such as the glove used by Okorokova et. al., generally focus on fingertip sensing due to the outsized impact on daily life of losing an upper limb [65]. Searching for a more accurate representation of the human sense of touch, Osborn et. al. pursued a neuromorphic fingertip e-skin design that replicates the functionality of mechanoreceptors and nociceptors in actual human dermis (Fig. 4i) [56]. Mechanoreceptors provide our general tactile feedback while nociceptors are specifically tuned to transmit painful sensations. The e-skin consists of two layers separated by silicone encapsulant, each containing an array of stretchable conductive fabric traces laid on top of a piezoresistive fabric. The top layer represents the nociceptors and was fabricated with half the number of sensing nodes in the bottom layer. This reflects the real balance of nociceptors to mechanoreceptors in human skin and is also accounted for in the feedback model. After mapping the feedback to his phantom limb through transcutaneous electrical nerve stimulation (TENS), an amputee user was able to easily identify touch with three different digits, distinguish between objects of varying shape, and execute a pain reflex coded into the feedback model. These results represent a major step towards more lifelike pressure sensing for prosthetics and expansion of tactile feedback features to cover all aspects of natural human physiology. In another study, Lai et. al. developed a self-powered pressure sensing skin based on triboelectric principles [83]. The sensing skin was fabricated by drop-coating Ag flakes into a thin matrix, then sandwiching the matrix between two silicone rubber layers. The device displayed remarkable mechanical and electrical stability under both 100% elongation and intense cyclic loading. In addition, the triboelectric skin achieved a sensitivity of 0.29 kPa^{-1} and was able to discern pressures as low as 63 Pa. In practical application, the sensor was adapted into a simple robotic gripper to complete object manipulation tasks. The recorded data clearly showed distinct voltage responses correlated to increasing and decreasing grip force, as well as full release of the object. Lastly, we will discuss indirect calorimetry. Indirect calorimetry (IC) traditionally serves as the gold standard in clinical metabolic analysis [105]. However, it can also be leveraged as a signal for integrated robotics and visual interfaces [10], [24], [25], [106], [107]. In such applications, gas sensors are sealed into portable mask-based systems that can measure a user's O_2 and CO_2 volumes. From this information, metabolic statistics such as respiratory quotient or energy expenditure can be calculated for implementation into control algorithms [108]. Additionally, IC is a great way to quantify the effect of assistive robotics and visual feedback. Recently, Kim et. al. utilized the Cosmed K5 wearable metabolic system to provide visual feedback during ankle exoskeleton training sessions, evaluating the efficacy of such feedback in user adaptation to exoskeleton parameter tuning [18]. Using the calculated metabolic cost, subjects were constantly updated on their ankle dorsiflexion/plantarflexion and given on-screen cues suggesting how to work more harmoniously with the exoskeleton. Subjects training with suboptimal exoskeleton parameters were actually able to adapt to the specific conditions and decrease their metabolic cost over the course of a session by responding to the feedback presented through the integrated visual interface. Additionally, Kang et. al. used metabolic cost to inform power delivery optimization of a hip exoskeleton [109]. An indirect calorimetry system was used as an evaluation tool to study four different levels of exoskeleton assistance. It was determined that delivering assistive torque between 13% and 26% of the peak biological hip moment provided the greatest reduction of metabolic cost. Studies such as these show how niche physiological signals can be adapted to

robotics and visual interfaces in unique ways to educate new users of wearable robotic systems. Additionally, metabolic cost derived through indirect calorimetry is a crucial tool for optimization of wearable robotics, making it possible to see greater adoption of such systems in the future.

2.5 Multifunctional Sensors

Recently, sensor research has evolved to introduce systems capable of targeting multiple signals. These systems tend to fall into one of two categories: those that include multiple sensors in one device for multimodal signal collection, and those that target one signal at a time but can be configured in different ways. Naturally, many systems of the first kind tend to be larger in size and more complex. For example, the mobile nursing robot developed by Mireles et. al. [21]. This robot seeks to provide automated health monitoring for senior citizens using an impressive suite of on-board sensors. These include ECG, arterial pressure, heart rate, oxygen saturation, and temperature. However, smaller multimodal sensing devices also exist, such as the unified IMU/EMG sensor presented by Zhao et. al. [110]. Arm position and muscle activation data collected with the IMU and EMG sensor, respectively, are fused to expand the library of recognizable gestures during control of a wheeled robot. Dindorf et. al. chose to combine EEG and EMG signals from a sensor headband to control a custom elbow orthosis. A unique control algorithm was tuned to classify the combined signals, driving a set of pneumatic artificial muscles providing assistive torque to the elbow joint for forearm flexion/extension [111]. On the other hand, devices in the latter group tend to focus on novel electrode designs that enable adaptation to different signal targeting areas. Zhang et al. present a unique dry electrode design suitable for measuring ECG, EMG, or EEG [112]. Using a combination of poly(ethylenedioxythiophene):poly(styrenesulfonate) (PEDOT:PSS), waterborne polyurethane (WPU), and D-sorbitol, the electrodes are able to reduce contact impedance and noise compared to commercial silver electrodes and previous examples in literature. In another study, Tian et. al. expand the applications of epidermal electronics by introducing a sensor array covering up to 40 times the area of existing devices [113]. Each array consists of 17 Cr/Au electrodes, created using traditional photolithography and encapsulated in polyimide and silicone layers. The large size (over 200 cm^2) and number of channels enables the device to reliably cover areas such as the entire circumference of the arm. The design successfully demonstrated multichannel EMG control of a transhumeral prosthesis (with classification accuracy of 89%), full-scalp EEG measurement by linking four devices, and compatibility with MRI equipment. Highly adaptive mechanical sensors with the ability to target many physical motions have also been designed recently. Wu et. al. show how a simple strain sensor can be used in a variety of different ways to provide insight into human motion [22]. A CO2 laser was used to directly pattern graphene serpentines from a polyimide film, then polydimethylsiloxane (PDMS) served as a transfer layer to peel the laser-induced graphene (LIG) off of the substrate (Fig. 5). The PDMS-encapsulated LIG sensor displayed excellent mechanical and electrical stability under large strains (70-80%) and cyclic application of smaller strains (20%, 1000 cycles). Demonstrations of HMI applications included joint angle measurements of the phalanges, pressure measurements at the fingertip, and even arterial pulse waveform measured at the wrist. Meanwhile, Zheng et al. applied a completely different working mechanism to develop a sensor with similar versatility [8]. Their device was based on triboelectric nanogenerator (TENG) technology, and thus boasts the additional benefit of being self-powered. The sensor can be used in multiple modes, targeting joint angles, simple gait detection, and respiratory cycles. A particularly unique application, personal identity verification, was demonstrated by detecting minute differences in the waveforms of two subjects making identical hand gestures. Finally, Pang et al. present a device that combines triboelectric and piezoresistive sensing principles to mimic the behavior of different mechanoreceptors [14]. The skin-inspired sensor consists of a CNT-based piezoresistive sensing layer (mimicking the sustained response of slow-acting mechanoreceptors) and a Teflon-infused textile triboelectric layer (simulating how fast-acting mechanoreceptors respond sharply to momentary contact)

stacked on a copper electrode base. Similar to previously discussed studies, many different signals were targeted using the same fundamental working principle. The sensor displayed excellent signal quality and mechanical robustness while measuring joint angles, arterial pulse waveforms, and even speech patterns when applied to the throat.

2.6 Additional Sensor Developments

The previous sections have presented recent sensors through the lens of modality, with a focus on highlighting demonstrations of integration with robotic systems and visual interfaces. Here, we will supplement the preceding discussion by reviewing several broader developments in sensor technology. These advancements can be applicable to biosignal-integrated robotic systems in the future. Over time, research in the separate spaces of sensors, robotics, and visual interfaces tends to cross-pollinate and unify due to significant overlap of applications. One area of sensor technology we hope to see integrated is the use of nanomaterials. A major advantage of nanomaterials is their ability to combine with polymers to form flexible electronics. Silver nanowires (NW) are popular due to their excellent conductivity and electrical performance in percolation networks. Jeong et al. used AgNW to demonstrate flexible pressure sensors with an air gap structure to increase sensitivity. Using a printed electrode base, AgNW sensing element, and PDMS encapsulation, the sensor displayed excellent cyclic stability and low hysteresis during measurement [114]. Kim et al. also used AgNW and PDMS in a two-layer strain sensor. The prestrained, electrically decoupled layers could sense multidirectional strain, which could be appliedn biosignal-integrated robotics at multi-DOF joints such as the shoulder or hip [115]. While initial synthesis of NWs can be time-consuming, the sensors are quickly fabricated by facile methods such as drop casting [114], [116]. Copper NW is another nanomaterial with excellent electrical properties and great potential for sensing biosignals. One major advantage of CuNW over AgNW is their reduced cost (around 100 times cheaper) for a minimal loss in conductivity [117]. However, a common problem that plagues CuNW is oxidation and subsequent degradation of sensing performance. Hong et al. have addressed this shortcoming by developing several encapsulation methods using polyethylene terephthalate, polyimide, and silicon oxides [117], [118]. Kim et al. have also demonstrated oxidation-resistant CuNW sensors for EMG, ECG, and capcitive touch sensing [119], [120]. Bang et al. build on this by introducing the reversible, selective laser-induced redox (rSLIR) method for fabricating electronics with a seamless metal-semiconductor interface. Along with smoothly integrating three different varieties of Cu-based NW, rSLIR is able to pattern detailed images into thin-film electronics, showing promise for future application towards biosignal detection and sensor-robotics integration [121]. Along with nanowires, nanoparticles (NP) are widely used in the fabrication of flexible, wearable electronics. Similarly to NW, metal NPs display good conductivity and are easily integrated with polymers, as well as other sensor materials. For example, Zhan et al. combined AgNPs with CNTs on a spun TPU/polydopamine mat to create a flexible strain sensor [122]. By using multiple conductive materials forming their own networks, the sensor achieved both a broad sensing range and high sensitivity. This was validated through strain measurements of a variety of human movements, from skin stretching during blood pulse to large-angle bending of the fingers, wrists, and legs. In a similar concept, Tsai et al. used AgNPs to enhance the conductivity and surface roughness of a polymer/paper-based piezoresistive pressure sensor [123]. Nanoscale patterning has been shown to increase sensitivity, a potential benefit in HMI applications using small-amplitude signals such as EMG-controlled robotics. Truly skin-like wearable sensors are also being developed using NPs. For example, Kim et al. have created a flexible, conformal, microscale thickness epidermal electronic system capable of real-time circuit optimization and sensor modification [124]. Meanwhile, Shin et al. use NiO NPs to demonstrate a wearable temperature sensor on a substrate just 25μm thick [125]. Devices such as these have significant potential in biosignal-integrated robotics applications, as their minimal form factor enables seamless combination with emerging low-profile and soft wearable robots.

Another area of sensor development with prospective relevance to biosignal-integrated robotics is transparent sensors. While the visual characteristics of a sensor may not seem important compared to its quantitative performance metrics, there are several reasons optical transparency is desirable in modern sensors. Especially relevant to wearable healthcare sensors is the fact that opaque devices obscure the sensing area. A transparent device preserves visual access to the target tissue and, combined with measured biosignals, enables us to create a full picture of the clinical situation [126]. Furthermore, along with high mechanical compliance, optical transparency helps sensors remain imperceptible during daily use. Not only does this alleviate concerns over visual obtrusiveness and help normalize the widespread adoption of wearable sensors, but it also improves immersion in extended reality applications [126], [127]. Won et al. present an excellent example of such a device. They use an ultra-stretchable kirigami structure based on a colorless polyimide substrate to demonstrate multiple biosignal sensing modalities. A proof of concept for HMI integration is also provided by using forearm EMG measurements to control a drone with hand movements [128]. Chen et al. take a different approach, using ionogel fibers as a transparent dielectric material for capacitive sensors [129]. The device displays excellent pressure and temperature sensing capabilities, making it and other transparent capacitive sensors a promising candidate for skin-like sensing in prosthetic HMI applications. Finally, we will briefly discuss recent progress in machine learning (ML) methods for the analysis of biosignals. Where flexible, stretchable, skin-compliant platforms represent the state of the art in biosignal measurement, ML forms their counterpart on the signal analysis side. ML algorithms are uniquely suited to biosignal-integrated robotics due to their excellent feature extraction capabilities and ability to learn or evolve over time [130]. For example, unsupervised methods such as contrastive learning can be implemented to train algorithms to adapt to new users or data features not featured in their original training data [131]. Examples of popular ML algorithms include deep learning models [132], [133], support vector machines [62], [134], and many types of neural networks [51], [135]. These frameworks have been used to analyze a variety of signals, from EEG and EOG to haptic touch, then turn and issue directives to robotic actuators and data visualization interfaces [130].

3. Robots

A robot interprets sensor inputs, implements control strategies, and performs an action to a specified objective [136], [137], [138]. This review centers on robots as the central component bridging sensors and visualization interfaces, collectively forming the bio-integrated robotic system designed for real-world applications. Viewed through a robotics perspective, this system is actualized through an array of control strategies, each built upon diverse sensory input modalities and output mechanisms. The yielded outputs can be channeled into either physical or non-physical interaction with users, including visualization interfaces, thereby fostering a symbiotic adaptation between humans and robots. Modern robots can take many forms, from small teleoperated drones to full-body exoskeletons. An important axis by which this wide range of robots is categorized is their flexibility, i.e., rigid vs soft robots. Most fully biosignal-integrated robotic systems still feature traditional rigid robotic structures and actuation. This section will focus on these rigid robots from a hardware perspective, but many of the control strategies discussed will also be relevant to soft robots.

3.1 Applications

3.1.1 Healthcare

Robots have found applications in the field of healthcare and rehabilitation as a result of the fusion between medical sciences and artificial intelligence [139]. These robots are designed for different tasks, from elderly and patient care to walking assistance, rehabilitation, and neurorehabilitation [140]. We describe three subcategories of bio-integrated robots in the healthcare field.

Wearable assistive robotics has emerged as a promising technology to assist humans in enhancing, supplementing, or replacing limb motor functions, commonly affected after suffering an injury, a stroke, or as a result of natural aging [141], [142]. Robotic prostheses and exoskeletons have emerged as important tools in wearable assistive robots with the aim of enhancing the quality of life for individuals facing limb loss or dysfunction. Those devices are designed to enhance functional mobility [143], independence [144], psychological well-being, and self-esteem [145]. For instance, individuals with transtibial amputation, the most prevalent form of amputation [146], frequently encounter balance-related challenges [68]. Such challenges can be mitigated by a robotic ankle-foot prosthesis, including one with two toes, enabling ankle inversion/eversion assistance in addition to the plantarflexion [68]. The effectiveness of the two-degrees-of-freedom ankle-foot prosthesis was shown by reduced foot placement control effort, physical exertion, and intact limb control effort [147]. Recent work showed that step-to-step modulation of inversion/eversion torque can reduce metabolic cost by 13% (Fig. 6a) [148]. Similar work further personalized the assistance from the device using human-in-the-loop optimization with an objective function of enhancing symmetry [12]. The approaches, however, still lack feedback to the user. BeBionic prosthetic hand (Ottobock, Duderstadt, Germany) equipped with the capability to perceive both touch and pain through a multi-layered e-dermis (Fig. 6b), presents the potential to create a more natural sensation encompassing various tactile stimuli for prosthetic hands [56]. For paraplegic patients, movement predictability when using exoskeletons is a challenge. Solutions using surface electromyography signals from the upper limbs show promise, with some reporting predictive accuracies of up to 80.75% across different subjects [77]. Care robots engaged in the process of patient care are often referred to as care robots. The major target populations for care robots are the elderly [149] and children [150] with mental disorders. These robots can offer both physical and mental assistance in the process of monitoring, diagnosing, and education [140]. Persistent challenges in social communication and interactions, as well as restricted and repetitive behavior patterns, have been observed in children with autism spectrum condition (ASC) [151]. The Personalized Perception of Affect Network (PPA-net) is a developed machine learning framework that adapts to a child's affective states and engagement across different cultures and individuals [96]. This robot-assisted therapy was implemented using a NAO social robot. Results indicate that integrating audiovisual and physiological expressions of affect and engagement reduced the issues of noise and missing data from children with ASC. A new architecture for human-humanoid interaction, centered on an EEG-brain computer interface (EEG-BCI), was designed specifically for patients with locked-in syndrome (ALS) [152]. This system discerns users' mental states using biofeedback factors such as attention, intention, and focus and employs a NAO robot to carry out tailored behaviors. Data indicates that ALS patients can effectively command a humanoid robot through this BCI design, potentially enhancing their capacity to manage daily tasks and engage with their surroundings. Care robots can collect physiological signals to assist in monitoring and diagnosis tasks. This requires secure and bidirectional communication between patients and healthcare providers [153]. For instance, a mobile nursing robot with a user-friendly graphical user interface is presented by Mireles et al. [21]. Nursing robots can monitor the patients's vital signs such as electrocardiography potentials, oxygen saturation levels, skin temperature, and non-invasive arterial pressure in home settings. In another operation mode, this nursing robot can help individuals with gait assistance. Care robots can be controlled with physiological signals. While brain-computer interfaces (BCI) were primarily used for controlling single devices such as wheelchairs [153], robotic arms [9], or prosthetic limbs [154], their scope is expanding. A hybrid BCI can manage both a wheelchair and a robotic arm, showcasing the growing versatility of BCIs in multi-task operations. The UL8W wheelchair and JACO6 DOF-S robotic arm system has been controlled using EEG and EOG signals (Fig. 6c-d) [155]. Wheelchair direction is determined by hand motor imagery, whereas eye blinks and eyebrow movements initiate commands for the wheelchair and robotic arm. Neurorehabilitation robots have been used in the rehabilitation field. Independent robotic

manipulators can measure the effects of simultaneous neuromuscular modifications [67]. To enhance the efficiency of neurorehabilitation exercises, a novel BCI framework was introduced, employing autoencoder-based transfer learning and a UR-5 robotic arm [87]. Experiments reveal improved EEG signal classification compared to state-of-the-art approaches. Marini et al. examined electrocortical dynamics of upper limb position matching task with and without vision feedback using a planar robotic workspace (Fig. 6e) [59]. A interactive musculoskeletal simulator (IMS) was developed by Hasson et al., permitting users to control a muscle activity-driven model of their arm [67]. A custom robotic interface is described to move the user's hand following the virtual arm model movements (Fig. 6f). By manipulating musculoskeletal dynamics in real-time, insights can be gained into neuromuscular system intricacies linked to injury, disease, and aging.

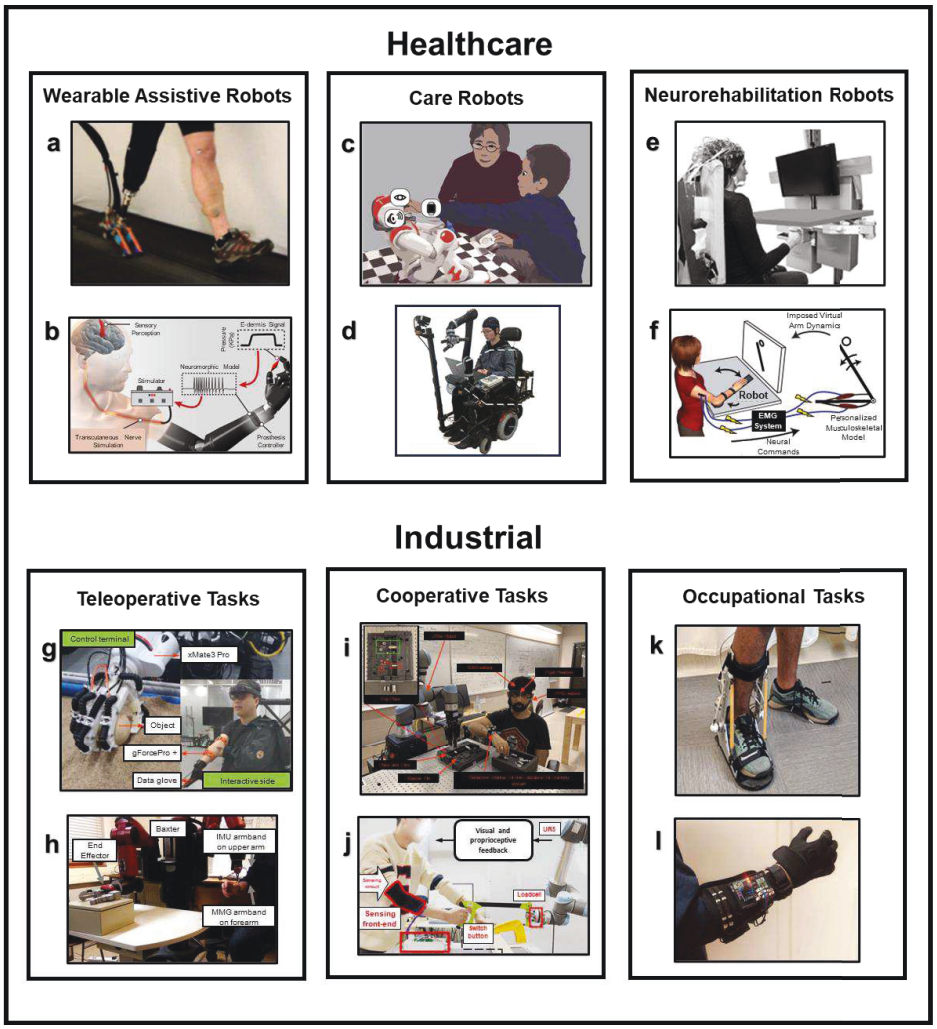

Figure 6. Applications of bio-integrated robotic systems. (a) Robotic ankle-foot prosthesis with two degrees of freedom, aiding level walking for transtibial amputees. Reproduced according to the terms of the CC BY license [148]. Copyright 2017, the authors, Frontiers Media SA **(b)** Prosthetic hand capable of tactile and pain perception via a multilayered e-dermis. Reproduced with permission [56]. Copyright 2018, AAAS. **(c)** A social robot offering ML-driven personalization of autism care. Reproduced with permission [96]. Copyright 2018, AAAS. **(d)** Innovative hybrid BCI using EEG and EOG to control an integrated assistive system, comprising a wheelchair and robotic arm. Reproduced according to the terms of the CC BY license [155]. Copyright 2019,

Frontiers Media SA. **(e)** Planar impedance-controlled robot, capable of measuring high-resolution trajectories in generated force fields. Reproduced according to the terms of the CC BY license [67]. Copyright 2019, PMC **(f)** Custom planar robot with interactive musculoskeletal simulator for matching arm and arm model movements. Reproduced with permission [59]. Copyright 2018, IEEE. **(g)** Wearable sensor-based motion capture for the human upper limb, facilitating teleoperation of an arm robot. Reproduced according to the terms of the CC BY license [156]. Copyright 2022, MDPI. **(h)** Gesture recognition through IMU and MMG sensors on both arms, controlling a Baxter Robot. Reproduced with permission [103]. Copyright 2019, Elsevier. **(i)** Framework enabling continuous data collection during Human-Robot Collaborative tasks when changing robot movements as a form of stimuli to invoke a human physiological response. Reproduced with permission [157]. Copyright 2019, IEEE. **(j)** Physical HRI that combined the electrical impedance tomography (EIT) based sensing approach with the robotic controllers to produce proper assistance with external uncertainties in the collaborative sawing task using a UR5 arm robot. Reproduced with permission [158]. Copyright 2021, IEEE. **(k)** Ankle-foot exoskeleton with two degrees of freedom and active plantarflexion for squatting assistance, utilizing ECG signal. Reproduced according to the terms of the CC BY license [12]. Copyright 2023, the authors, Springer Nature. **(l)** Reliable single EMG-based control of a portable robotic glove, identifying power grasp for augmenting the grasping force. Reproduced according to the terms of the CC BY license [70]. Copyright 2021, IEEE.

3.1.2 Industrial

Industrial robots played a prominent role in the development of industry in the past decades. Industry 4.0 prevalence introduces more complex and flexible tasks. In order to meet these demands, industrial robotic systems need to be more independent and intelligent [159]. Robot teleoperation is defined as "controlling a robot that may be at some distance from the operator" by Nielsen et al. [160].Teleoperation technology has been used in diverse industries, such as space exploration [161], [162], military [163], under-water exploration [164], hazardous environments [165], and oil and gas explorations [166], [167], [168]. Bio-integrated teleoperation robots harness the cognitive and physiological signals of humans to assist robots in making critical decisions [169]. By integrating this technology with advanced visualization methods, a collaborative environment can bridge the user and robot [170]. The gForcePro+ armbands were used to construct a kinematics model of the human arm (Fig. 6g) [156]. By applying surface electromyography (sEMG) to counter physiological tremor effects, the model was evaluated with the xMate3 Pro robot. The outcomes indicated enhanced teleoperation tracking and reduced tremor. Another investigation introduced a headset that captures eye movement and facial expressions to control a DJI Spark drone [171]. A hexapod robot also has been controlled using another BCI interface [60]. Further research employed a Mechanomyography (MMG) gesture recognition system [103]. This system integrated six unique analog control signals, corresponding to the 3D Cartesian coordinates from each hand, to operate a Baxter robot (Fig. 6h). A study explored the use of a biologically-inspired multimodal human-in-the-loop control system for a pneumatically actuated robot arm, focusing on a hammering task [172]. This findings suggest the system's effectiveness in autonomously deriving robot skills for tasks requiring precise motor control. Collaborative tasks have been utilized to enhance productivity [173] and operational efficiency [174], [175]. Therefore, creating collaboration tasks between humans and robots which requires intuitive [176], [177] and safe [178], [179] human-robot interaction. Physiological signals can be used to inform such systems of humans' mental [180]or physical state [93]. Visualization, on the other hand, can provide visual cues in the shared human and robot working space, creating human-aware behaviors of the robotic system [181]. Robots in human-centric environments can lead to unpredictable physical interactions, known as active physical human-robot interaction (APHRI). The nuances of human perception and the safe management of these interactions are

still under exploration. To better understand this, Hu et.al., were engaged in a visual game with a Sawyer arm robot, where they encountered tasks triggering active physical interactions [93]. Recognizing the importance of understanding human states for optimal human-robot collaboration, machine learning techniques were employed to interpret interaction parameters from the upper body's sEMG signals [11]. A convolutional neural network (CNN) was utilized to predict motor control difficulties during a physical human-robot interaction (pHRI) using a Schunk Powerball LWA4P arm robot. This model was further adapted to new subjects using a transfer learning approach. To deliver to operator intentions and manage unpredictable external factors in human-robot collaboration, a novel control interface was introduced [158]. It integrated electrical impedance tomography (EIT) sensing with robotic controllers. By leveraging optimized EIT features, the interface estimated forearm muscle contractions, using a wearable fabric band for ease. This solution was validated in a human-robot sawing task and hints at its use in wearable robots assisting hand movements (Fig. 6i-j). Industrial human-robot interaction (HRI) primarily focuses on human safety, trust in automated systems, and productivity enhancement [182]. In this context, it is important to create event markers for both humans and robots and to ensure data synchronization during interactions [157]. The study aimed to understand how the acceleration and path of UR5e and UR10 robotic arms influence human physiological responses during joint tasks (Fig. 6i-j). It also evaluated human responses under varied safety algorithms in these collaborations. As the industry grows, occupational safety grows as a common concern with it worldwide. Addressing this challenge, automated and robotic systems can help prevent or reduce occupational injuries and create safer workspaces for workers [183]. Beyond medical applications, exoskeletons also offer potential in occupational settings. They can provide assistance and reduce workplace injuries [184], [185]. In this context, the utility of a biopatch becomes evident. This patch measures vital indicators such as heart rate and computes the RMSSD, serving as a method to estimate metabolic cost (Fig. 6k) [12]. The Exo-Glove Power (EGPO) is a bowden cable-driven robotic glove. Its purpose is to enhance the grasping force when users exert a strong power grasp on an object (Fig. 6l) [70]. The EGPO utilizes a single EMG sensor-based myoelectric interface to identify the user's grasp intention, offering a reliable and intuitive mechanism. Unique biological features of the musculotendinous junctions allowed two myoelectric control methods for robotic glove-dual-threshold control and morse-code control.

3.2 Control Strategy

Achieving precise and efficient control over complex robots is necessary for their successful operation [186]. To address this challenge, a hierarchical approach known as the hierarchy of control has emerged as a framework for robot control [187]. In this section, we categorize the most prevalent control strategies employed in biosignal-integrated robotic systems.

3.2.1 High-level control

In the hierarchical structure of robotic systems, the high-level control layer takes center stage, functioning as the cognitive core (Fig. 7). Here, strategic decisions and objectives are shaped by sensor data and human input, addressing mission planning, task allocation, and decision-making [188]. The integration of physiological sensors and the human-in-the-loop concept enables the controller to receive both physiological and non-physiological feedback, enhancing precise robot control [31], [189]. Commands from this layer are relayed to mid and low-level controllers. For example, a BCI-driven upper body exoskeleton may utilize a wearable fPCB as its control hardware. This fPCB could contain an analog-to-digital converter circuit, power circuit, and microcontroller. The high-level control software's job would be to take in a raw biosignal, filter it, convert it to a digital signal, and then analyze it to generate a command consistent with the user's intention. For example, "close the left hand." This is passed on to the control software's mid- and low-level blocks for execution.

Movement and gesture recognition selects its action output automatically based on the user's movements or intended actions. The primary advantage of this approach is its ability to operate without imposing any cognitive load or requiring direct input from the user, thereby enhancing the intuitiveness and naturalness of the interaction [190]. Various sensors, both physiological and non-physiological, or a combination of both, can be employed to detect body movements and gestures. The most commonly employed methods include muscle activation (EMG), spatiotemporal sensors (IMU and encoders), and haptic and pressure-based measures. Antonelli et al. employs a model-based approach to generate a control signal for executing a desired pick-and-place task with a robot [16]. It involves the collection of surface EMG signals from three fingers, which are subsequently processed and sent to the action block for controlling a pneumatic muscle. Huang et. al., presented a continuous control scheme for effective management of an upper-limb prosthesis . This system employs eight channels of EMG signals from the human upper limb, which model and regulate reach and grasp functions of the prosthesis. Its operation is based on model recognition control with an emphasis on the central processing unit (CCU). After fulfilling model identification criteria, the relevant characteristics are extracted from the raw EMG signals, enabling the establishment of desired speeds and grasping configurations. This study indicates the necessity of defining the intentional control state and the unintentional control state explicitly before implementing the continuous control scheme[15]. Myoelectric control has also been investigated, mapping EMG features to prosthetic digit positions, specifically for the Prensilia IH2 Azzurra hand [71]. Another study integrated a blend of implanted epimysial EMG and surface EMG to manage a 12 K50 elbow and VaryPlus Hand for tasks linked to grasping and transferring [73]. The nonnegative matrix factorization (NNMF) method was employed to extract synergies from sEMG signals, leveraging its nonnegativity constraint. These extracted synergies were subsequently used for decoding intention and operating a bionic neuroprosthetic arm [191]. For enhancing the biological control interface of myoelectric prostheses post above-elbow amputation, targeted muscle reinnervation (TMR) was explored. This method found that surgical nerve rerouting could achieve selective activation of muscle units, leading to a multitude of independent myoelectric control signals. sEMG biofeedback was used to train the activation of these new muscle units, facilitating the creation of up to six control signals for a tabletop hand prosthesis [74]. Physiological sensors can provide valuable insights into human states or intentions. However, limitations such as slower convergence, extended processing times, or the body's delayed physiological responses can be restrictive for certain robotic applications. As a result, combining physiological with non-physiological data is sometimes more effective. Beck et al. suggest that for optimal balance in exoskeletons, reactions should be faster than physiological responses [81]. To achieve this, metrics such as center of mass (CoM) kinematics, which are faster than physiological responses, are recommended to generate control commands. Another research introduced a controller utilizing a finite state machine model, focusing on weight shifts between feet to produce gait trajectories. This controller was applied to the MOTION exoskeleton [20]. A symmetric foot force-time integral (FFTI) has been presented as a cost function to optimize stiffness in the control of an ankle-foot prosthesis [106]. For the position control of a Baxter arm robot, a combination of IMU and mechanomyography (MMG) sensors was employed to detect arm gestures and transmit commands to its lower components. This method generated six analog control signals, corresponding to the 3D Cartesian coordinates of the hands, supplemented by a discrete control signal initiated by right-hand gestures [103]. In another approach, a hybrid mix of facial haptic feedback, sEMG signals, and IMU data was employed to produce multiple high-level commands for a CyberLimb arm and hand prosthesis [26]. Eye and facial gesture recognition has been showcased as a novel method to navigate a telepresence drone, emphasizing its intuitive nature [171].

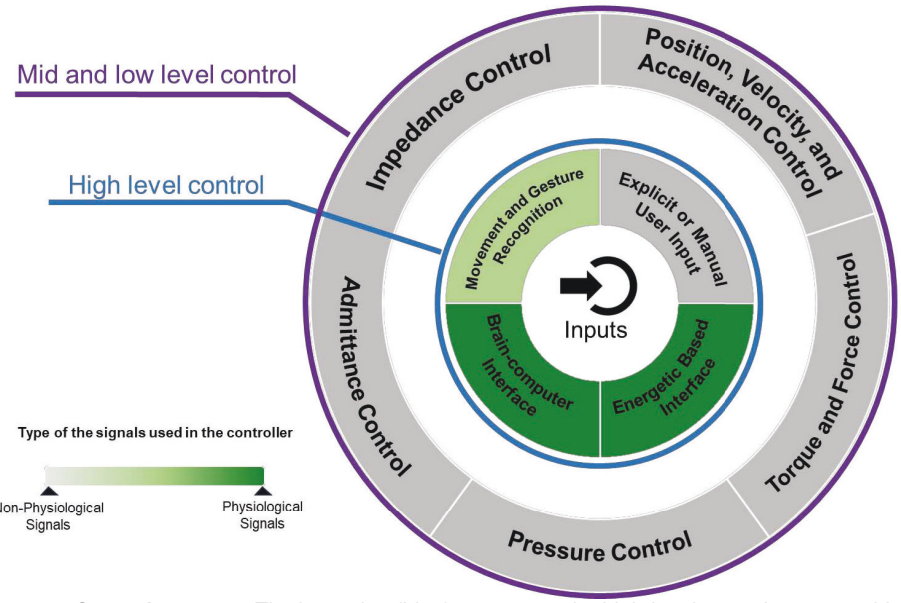

Figure 7. Control strategy. The inner ring (blue) represents the high-level control strategy which defines the overall behavior of the robotic system. Inputs to this high-level controller may originate from the user through input devices and/or sensors. The outer ring (purple) portrays the mid and low-level control strategies. This layer dictates device-specific, continuous behaviors of the robotic interface. The color gradient signifies the varying utilization of physiological and non-physiological signals across control strategy categories and layers.

Brain-computer interface (BCI) technology represents an approach to information exchange, translating brain-generated signals into machine control commands [192]. The most common BCI signal is the motor imagery (MI) electroencephalography (EEG) signal, owing to their spontaneity and device independence characteristics. The main steps in the BCI control process are signal acquisition, preprocessing, feature extraction, and classification [193]. Several advances in EEG signal outcomes have been utilized for robotic control. For instance, a KUKA robotic arm can be controlled using a binary coding method, which interprets four MI-EEG signals. This approach allows the robotic arm to have seven degrees of freedom, highlighting its intricate control mechanism [44]. Robotic aids for rehabilitation and assistance to those with physical impairments have also been a focus. A BCI, for example, integrates with a robotic hand orthosis specifically designed for stroke patients. Upon detecting motor intention in a paralyzed hand, the system sends a Bluetooth command to the ReHand orthosis. This device passively moves the paralyzed fingers, suggesting a promising direction in restoring motor functionality [45]. Similarly, an EEG helmet has been developed to transmit control signals to the PRISMA hand 1 prosthetic, aiming to improve mobility for those with upper limb amputations [61]. Stress mitigation in robotic interaction has also been examined. During a hybrid Brain-Neural Computer Interface (hBNCI) experiment involving a whole-arm exoskeleton, it was found that using EEG-based control resulted in higher stress levels and mental workload compared to using EoG control [55]. Further integration of technologies has led to the development of a hybrid BCI system. This system, which

merges Electrooculography (EOG), Steady State Visually Evoked Potential (SSVEP), and Motor Imagery (MI) inputs, effectively manages a rehabilitation interface, consisting of a UR-5 arm robot and a three-finger Barrett hand [87]. An innovative aspect of such integrations is seen in a hBNCI. This interface uniquely combines EEG and EOG to control a system comprising a wheelchair and a robotic arm, allowing users to navigate and send commands via motor imagery and specific eye movements [155]. In another direction towards merging human activity with robotic assistance, a comprehensive analysis of human walking has resulted in the creation of a Human-Machine Interface (HMI). This system captures electromyography signals from upper limbs and EEG signals during exercise. Such decoded signals then control a lower limb exoskeleton robot, translating user intent into action [194]. Additionally, the exact gaze direction of an individual, ascertained using the SSVEP brain response to visual stimuli, has been employed to steer a user interface for an assistive self-feeder robot [47]. These studies collectively showcase the vast potential of EEG-based controls in robotics and rehabilitation.

Metabolic cost emerges as a compelling metric for evaluating user performance and holds potential for application in rehabilitation and assistive robots [189]. Inspired by the biological principles of energy conservation and efficiency seen in living organisms, researchers are increasingly focusing on developing control methods that enable robots to manage and optimize user's energy consumption [195]. Since the early 2000s, researchers have actively pursued the development of lower-limb exoskeletons to enhance human mobility, with a primary goal of reducing the metabolic cost associated with walking and running when compared to locomotion without such devices [196]. For instance, Human-in-the-Loop (HIL) optimization with the covariance matrix adaptation evolutionary strategy (CMA-ES) have been used to pinpoint optimal energetic points for controlling an ankle exoskeleton [25]. Similarly, for squatting tasks, Bayesian optimization combined with HIL techniques has been employed to develop personalized assistance [12]. One of the challenges posed in these studies is the metabolic cost estimation. Traditionally, respirometry is considered the benchmark for such estimations. Researchers have focused on accelerating the convergence process such as a phase-plane based estimator of steady state metabolic cost [197] or Kalman filter with stopping process [198]. Yet, this method is hampered by the need for a cumbersome and rigid measurement apparatus, which reduces its practicality in field applications [12]. To address this, alternative approach has been introduced, such as energy expenditure estimation through heart rate variability, specifically the root mean square of successive differences (HRV-RMSSD) [12]. Other methods for metabolic cost estimation during squatting with an ankle-foot exoskeleton were investigated such as muscle synergy [24] and foot pressure measurements [10].

Explicit or manual user input selects the operational mode of the robot based on the user's direct inputs through buttons or voice commands. Due to their ease of implementation, high predictability, and reduced risk of errors, this method is sometimes preferred over other complex control methods. However, these advantages come at the cost of requiring increased user participation, resulting in a less natural user experience, heightened cognitive load, and potential operational slowdowns [190]. This control strategy often involves the collection of physiological signals rather than physiological-based control. A mobile nursing robot features multiple functions, with user commands provided through a GUI, which are then relayed to the robot's controllers [21]. The Pepper humanoid robot is equipped to recognize emotions in children with hearing disabilities. Children's responses on a tablet activate the robot's behaviors, with the robot reacting to correct answers. An Empatica E4 wristband and a camera collect physiological and facial data [19]. The EKSO GT is an active exoskeleton for gait rehabilitation, offering several operation modes. Actuation methods include button input from a therapist, buttons on crutches or a walker used by the patient, or the patient's body weight shifting and movement [199]. Another method controls the EKSO exoskeleton through manual input, utilizing collected EMG and robot sensor data to adjust the robot's functions [200]. Lastly, a knee exoskeleton employs a servo-controlled

mechanism to apply resistance during walking, beneficial for rehabilitating individuals with neuromusculoskeletal injuries [66].

3.2.2 Mid and low-level control

Following the high-level control, the mid and low-level control layers act as the action block of the control strategy (Fig 7). This layer is responsible for translating high-level directives into precise, real-time commands that the robotic hardware can execute [190]. Revisiting the example from Section 3.2.1, a command such as "close the left hand" is broken down at this level into instructions for individual hardware components to follow. Actuators in the wrist and fingers will need specific directions on actuation sequence and duration. The power delivery system requires guidance on where, when, and how much current to deliver. Translating high-level commands and delegating executables to different hardware elements is the ultimate task of the mid and low-level control software. This layer includes a wide range of functions, from trajectory planning and motion control to sensor fusion and feedback control [201], [202]. Mid and low-level controllers ensure that the robot's movements and interactions with its environment are executed with precision and adaptability [203]. We have categorized this layer into five categories. Position control is one of the common low-level control strategies [203], [204]. An advantage is its compatibility with various types of actuators, making it easy to integrate into diverse robotic systems and industries [60], [110], [157], [158], [205]. While position control offers substantial benefits, there are limitations to the method. Most electric motors have poor torque density, therefore, they need to operate at high speed to generate high power output. This conversion is often achieved through a high gear ratio which incearses the reflected inertia. In case of an unexpected contact, the shock response could result in damaging and unsafe movements [206], [207] Force and torque control is another common low-level control strategy in robotics, enabling robots to precisely regulate the application of force and torque in their interactions with the environment [208]. While they offer significant benefits such as real-time contact sensing and adaptability to dynamic surroundings, they also pose challenges, often requiring more complex joint-level design due to the usage of force sensors, which can lead to increased manufacturing costs and complexity [209]. Force and torque control find extensive application in rehabilitation robotics, including exoskeletons and prostheses, when designing assistive or resistive torque profiles [66], [109]. Impedance control, as extensively used in fields such as rehabilitation robotics and human-robot interaction (HRI) systems [97], [210], and human motor learning research [211], [212]. Impedance control focuses on dictating the stiffness and damping properties of the robot, allowing it to maintain a predefined trajectory and resist deviations caused by external forces, making it suitable for precision tasks such as manufacturing [213], [214], [215]. Using this method, controller can physically interact with users as active components. In impedance control, the robot's behavior is configured with parameters such as stiffness, damping, and inertia to ensure compliance with the user or the environment, delivering assistance or resistance torque when deviations from the intended movement are substantial [190]. It functions as a means to manage muscle stiffness to accommodate interaction forces, regulating the force exchanged between the robot and the environment. However, it's crucial to note that improper adjustment of impedance filter parameters may lead to unstable contact and excessive pressure on the target environment, emphasizing the importance of precise parameter tuning [2], [190]. Admittance control and impedance control represent distinct approaches to regulating a robot's interaction with its environment. Admittance control emphasizes controlling the robot's compliance and flexibility in response to external forces. Tracking external forces while providing significant assistant torque makes this controller suitable for rehabilitation studies [2], [216], [217]. Hence, admittance control is advantageous in applications requiring safe human-robot collaboration [11], [158], interaction with deformable objects, or tasks in uncertain and dynamic environments. However, high cost due to implementation of force sensors in the joint and trajectory instability due to external noise or contact with a rigid body can limit its use [2], [216], [218]. The choice between these control

strategies depends on the specific requirements of the task, with impedance control prioritizing precision and admittance control emphasizing adaptability and safety. Pressure control has employed in various pneumatic systems, including those using McKibben-type pneumatic artificial muscles (PAMs) [16], [50], [219]. This control approach centers on the regulation of compressed air pressure within these systems. By managing the air pressure, pressure control enables the safe actuation of pneumatic components, making it a key driver in robotic applications in rehabilitation [16], [44], where controlled and precise movements are essential. However, the system is often challenged to maintain precise pressure levels over extended periods due to issues such as air leakage, temperature variations, and limited response time [220], [221].

4. User Interfaces

The intersection of biosignal-integrated wearable robotics and user interfaces is foundational for human-machine synergy. As technology evolves, so too do the demands and expectations of users, leading to a diversifying landscape of interfaces. Recent literature highlights this transformation, revealing a gradient of interfaces that range from traditional lab settings to sophisticated augmented reality platforms. Interface design is ultimately driven by the specific application the system is intended for. This determines what type of interface hardware to use and which information is critical for the UI to display. Especially relevant to biosignal-integrated wearable robotics is feedback – visual cues and status indicators to update the user on key changes in a dynamic environment. Above all else, however, an easy-to-use interface tends to be the most successful. This incorporates visual clarity, consistency in navigation and organization, and simplicity. Current research in biosignal-integrated wearable robotics recognizes the key role of user interfaces and is adapting to develop best practices for their design further. Fig. 8 visually represents these interfaces, plotted within quadrants, delineating their integration with robots and sensors. This categorization offers a clear snapshot of the current interface ecosystem, showcasing varying complexity and integration. This section will further delve into three prominent categories: basic lab GUIs, mobile apps, and extended reality platforms.

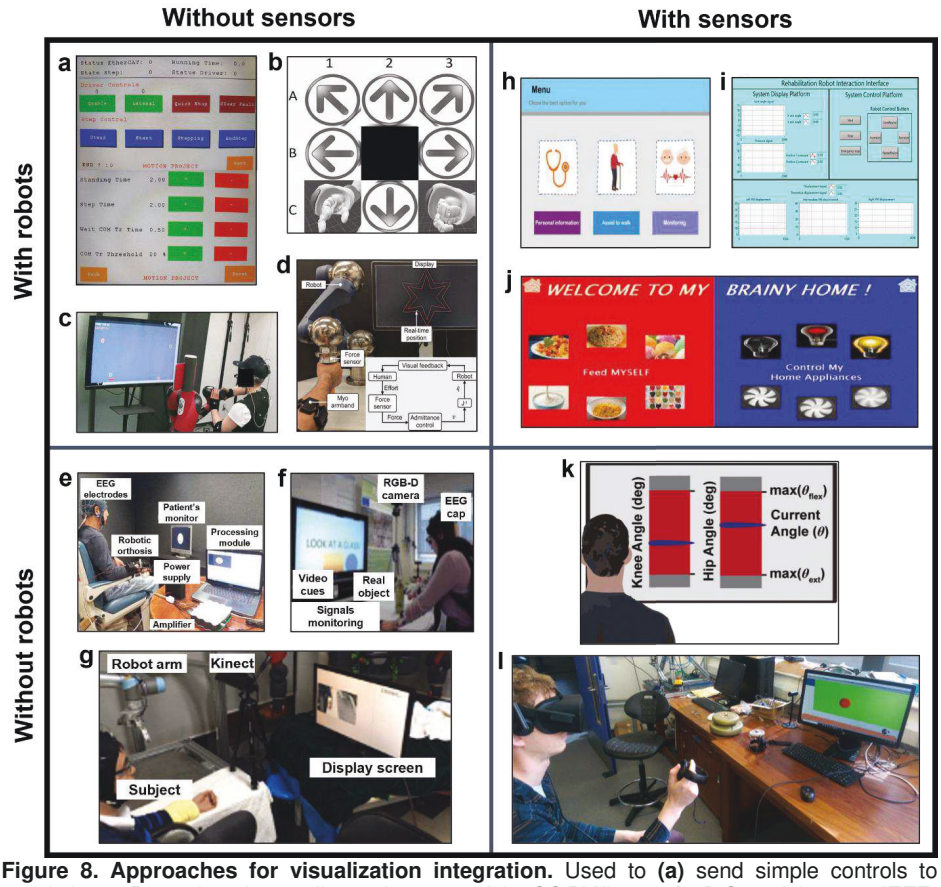

Figure 8. Approaches for visualization integration. Used to **(a)** send simple controls to exoskeleton. Reproduced according to the terms of the CC BY license [20]. Copyright 2021, IEEE, **(b)** send low level behaviors (e.g., directional control) and high-level behaviors (e.g., grasping control) to robot. Reproduced with permission [152]. Copyright 2017, IEEE, **(c)** match orientation of visualized puzzle pieces to the rotation of robot control arm. Reproduced with permission [93]. Copyright 2022, IEEE, **(d)** provide real-time position information on robot end-effector. Reproduced with permission [11]. Copyright 2022, ASME, **(e)** enable visual feedback on correct identification of motor intention. Reproduced according to the terms of the CC BY license [45]. Copyright 2021, Frontiers Media SA, **(f)** provide reliable assistance to grasp a real object. Reproduced according to the terms of the CC BY license [55]. Copyright 2019, MDPI, **(g)** show real-time content acquired by a Microsoft Kinect camera. Reproduced according to the terms of the CC BY license [87]. Copyright 2019, Sage Journals, **(h)** to display real-time physiological signals (e.g., ECG, oxygen saturation, and corporal temperature) and select robot modes for assistance. Reproduced with permission [21]. Copyright 2022, Springer Nature, **(i)** to control robot response movement and visualize real-time physiological signals (e.g., joint angle, plantar pressure, and pneumatic muscles). Reproduced with permission [219]. Copyright 2018, IEEE, **(j)** enable robotic assistance (e.g., feeding) and control of home appliances via EEG signals.

Reproduced with permission [47]. Copyright 2018, IEEE, **(k)** provide real-time feedback of hip and knee joint angles as bar plots. Reproduced with permission [66]. Copyright 2021, Elsevier, and **(l)** control the location of the virtual balls using IMU sensors. Reproduced according to the terms of the CC BY license [103]. Copyright 2019, Elsevier.

4.1 Basic lab GUIs

In the realm of biosignal-integrated wearable robotics, traditional screen-based graphical user interfaces (GUIs) remain an integral tool. Out of the papers reviewed in this category, many emphasized the importance of GUIs that are either directly embedded onto the robotic system or presented through dedicated computer applications. Such interfaces, primarily designed for lab settings, are appreciated for their precision, real-time feedback mechanisms, and adaptability.The integration of GUIs in healthcare and rehabilitation settings is paramount [222], enhancing both patient experience and clinical outcomes. Mireles et al. recognized the significance of real-time data, employing Matlab's GUIDE-based GUI to offer immediate clinical insights [21]. Similarly, Cantillo et al. incorporated a Bluetooth-enabled command mechanism in a robotic hand orthosis, providing empathetic feedback via facial expressions on a screen [45]. Uluer et al. introduced a custom GUI that synergized with a humanoid robot to facilitate interactive audiometry tests for children with hearing disabilities [19]. Li et al. developed a Windows 10-based control software for an exoskeleton, decoding motor intent from EEG and sEMG signals with 99% accuracy, exemplifying the seamless blend of biosignals and robotics in modern rehabilitation [194]. Exoskeletons, as extensions of the human body, require interfaces that ensure intuitive human-robot interactions. Zhang et al. presented a pediatric lower-limb exoskeleton, accentuating the importance of a GUI accessible via both a host PC and touchscreen [20]. Ai et al. employed a GUI for an ankle rehabilitation robot, aiding therapists in formulating rehabilitation strategies [219]. Kim et al. explored the influence of visual feedback on users of a robotic ankle exoskeleton [18]. Through a dedicated GUI, users received real-time visual guidance on walking patterns, emphasizing the pivotal role of GUIs in optimizing human-exoskeleton synergy. In experimental settings, GUIs play a crucial role in standardizing procedures and ensuring replicability. Shi et al. [223] and Batres-Mendoza et al. [60] employed GUIs to streamline and inform experimental flow. Shao et al. implemented a GUI-based simulation enabling users to control a virtual robot through EEG [224]. Hu et al.'s 2022 study leveraged a gamified GUI, allowing users to interact physically with a robot through a visual game [93]. Krasoulis et al. emphasized the significance of real-time feedback in myoelectric control research, using a GUI to guide participants in mimicking specific hand motions, underlining the crucial role of GUIs in real-time experimental validation [71]. Adaptable GUIs, tailored to specific user needs, hold immense potential in diverse applications. Vita et al. [225] and Sorbello et al. highlighted the necessity of adaptive interfaces for specialized user groups, such as children with ADHD or patients with ALS [152], [226]. Tabbal et al. introduced a versatile GUI that seamlessly transitioned between robotic arm control and managing home appliances, exemplifying the vast potential of GUIs in bridging the gap between healthcare and everyday life [47].

4.2 Mobile applications

In the contemporary digital era, the proliferation of mobile devices such as smartphones and tablets has engendered a paradigm shift in interface mechanisms for wearable robotics. The work by Leng et al. exemplifies this evolution [38]. This research delineates the integration of a mobile application with wearable robotic systems via Bluetooth connectivity. This interface elegantly translates user commands, such as "play", "previous song", and "next song", underscoring the convergence of routine user interactions with the complexities of robotic systems. Furthermore, Seppich et al.'s research elucidates the transformative potential of mobile devices in the realm of robotic prosthetics [26]. By leveraging the Samsung Galaxy S3 as a control interface, the study

accentuates the pivotal role of ubiquitous mobile platforms in facilitating intuitive and seamless human-machine interactions.

4.3 Extended reality

The immersive nature of extended reality, encompassing both virtual and augmented reality, offers a fresh perspective on user interfaces. The papers in this domain showcased the prowess of three-dimensional, simulated environments that can emulate real-world scenarios, be it for training, visualization, or therapeutic purposes. For instance, the work of Yeung et al. delves into a virtual experimentation realm where participants navigated a two-dimensional space, engaging with targets through varied controllers [227]. This exploration underscores the vast potential of virtual environments in enhancing user feedback mechanisms and fostering interactivity. Further emphasizing the immersive capabilities of XR, Wang et al. introduced an approach wherein real-time imagery from drone-mounted cameras was relayed to virtual reality headsets [171]. This integration not only facilitated an enriched visual experience but also harnessed human facial expressions and ocular movements to control the drones, accentuating the symbiotic relationship between user and machine. Zhu et al., while not elaborating on the specific intricacies of the interface, underscored the significance of immersive feedback within virtual environments [156]. Such feedback mechanisms, especially in the context of wearable robotics, serve to augment user experience and inform real-time interactions. Wilson et al. ventured into the domain of immersive robot teleoperation, leveraging virtual reality to ascertain the potential applications of IMUs [103]. The study highlighted the role of XR in expanding the horizons of experimental methodologies and user engagement. Li et al. delved further into teleoperation, integrating augmented-reality glasses with a reinforcement learning algorithm to carry out multi-robot collaboration [228]. In summation, the user interfaces in biosignal-driven wearable robotics are undergoing a transformative phase. As evidenced by the categorizations in Table 1, a substantial portion of the reviewed literature integrates aspects of visualization, robotics, and sensors. As technology continues to evolve, so does the canvas on which human-machine interactions are painted. These interfaces, whether they are traditional GUIs, mobile apps, or immersive extended reality platforms, are testimonies to the field's commitment to user-centric designs. Future endeavors in this domain will undoubtedly prioritize the fusion of functionality with an unparalleled user experience.

Table 1: Categorization of PRISMA-reviewed articles in biosignal-driven wearable robotics.

Reference(s)	Includes Sensors	Includes Robotics	Includes Visualization
[18], [19], [21], [26], [45], [47], [48], [55], [58], [59], [60], [62], [71], [78], [83], [86], [87], [88], [89], [133], [134], [156], [171], [191], [194], [219], [223], [227]	✓	✓	✓
[1], [2], [3], [4], [5], [6], [7], [8], [9], [10], [12], [14], [15], [16], [17], [22], [23], [24], [25], [39], [42], [44], [46], [50], [51], [52], [53], [54], [56], [57], [61], [64], [65], [67], [68], [69], [70], [72], [73], [74], [75], [76], [77], [79], [80], [81], [82], [95], [96], [97], [101], [104], [106], [107], [109], [110], [111], [112], [113], [155], [157],	✓	✓	

[158], [172], [196], [199], [200], [205], [225], [226]			
[38], [43], [66], [103], [135], [224]	✓		✓
[11], [20], [93], [94], [152], [228], [229]		✓	✓

5. Future Directions and Conclusion

Exciting new techniques for biosignal-integrated robotics systems are emerging, utilizing novel materials, control strategies, and fabrication techniques. Of particular interest is the development of new visualization methods, which bridge a critical gap in traditional HCI/BCI technologies by actively engaging the human user in an aware and active part of the signal path. In this new era of research, biosignal-integrated robotics with visualization are being designed with harmony as the guiding principle. This entails making design choices for constituent components with the overall system's performance as the primary evaluation platform. This may involve deviating from traditional designs and manufacturing techniques to further enhance biosignal quality, optimize robot design and control, and leverage the numerous capabilities offered by visual interfaces. Despite the progress, many challenges persist in seamlessly integrating human biosignals, robotics, and visual interfaces. For example, power delivery is expected to become a significant concern for certain wearable systems in the near future, particularly as they transition from lab environments to field use. Fixed power cables and stabilization equipment will no longer be feasible options. Complex wearable systems like exoskeletons will need slimmer and lighter form factors to provide practical benefits to most users. This will necessitate optimizing power consumption, battery design, structural component strength-to-weight ratios, and other factors. Personalization of robots is yet another complex challenge that must be addressed to enhance effectiveness and usability, especially in assistive robots. While integrating biosignals and robotics poses its own set of obstacles, the visualization aspect adds a layer of complexity. Ensuring real-time, intuitive, and unobtrusive visual feedback is crucial for user comprehension and interaction efficacy. Striking the right balance between the richness of visual data and the cognitive load it imposes on the user is essential. Optimizing display technologies for power efficiency, outdoor readability, and adaptability to varying user needs is essential. The landscape of future applications of the systems reviewed here is incredibly diverse and rapidly expanding. We anticipate that popular existing use cases, such as rehabilitation devices, will continue to be in demand as advances in sensors, robotic performance, and visualization technology improve their efficacy. Other clinical applications also stand to benefit from these developments. Examples include communication systems, environmental manipulation robots for patients lacking muscular control, and assistive robots for surgical procedures. In the foreseeable future, the evolution of human-in-the-loop control for robotic systems will be characterized by adopting sophisticated and hybrid control strategies, harnessing and analyzing multiple physiological and non-physiological signals. Additionally, some emerging cases aim to identify highly correlated alternative physiological or non-physiological measures, enabling the estimation of the original measure, thereby enhancing robotic systems' portability, usability, and speed. These advances may enable future devices to be deployable in the field in numbers not yet achieved. For example,

exoskeletons to assist manual labor in warehouses, factories, and construction sites could reduce occupational injuries and increase productivity for thousands of workers worldwide. Less common applications, such as nursing robots, may see expanded adoption as our society increasingly accepts human-robot interactions in daily life. New social robot designs could offer telemedicine, package delivery, and customer service improvements. New applications could represent fertile ground for significant expansion in biosignal-integrated robotics. The defense industry, for instance, is a major potential player in this arena. For example, the United States Army has recently completed trials of the Microsoft HoloLens mixed-reality goggles and is poised to adopt a custom system version [230]. Commercial wearable sensors are already being tested to monitor troops' vital signs and stress levels [231]. Robots have long been utilized for military situations requiring enhanced range, speed, and precision (e.g., unmanned aerial vehicles) [232] or tasks too hazardous for troops (e.g., disposal of unexploded ordnance) [233]. A natural progression appears to be sharing data between these elements for seamless communication within an integrated system. Biosignal-integrated robotics continuously evolve to achieve higher performance and cater to a wider variety of users. Recent developments include novel nanomaterial-based sensor designs, incorporating metabolic cost into robotic control, and integrating new XR visualization techniques. This review has divided integrated systems into three distinct components: sensors, robotics, and the emerging field of visual interfaces. Physiological sensing encompasses the measurement of potentials generated by the human body, such as those arising from natural bioelectrical currents or mechanical deformation. The design space of physiological sensors is expanding to encompass accurate devices applying novel materials and synthesis methods, improving skin conformality, reducing noise and interference, and enhancing breathability. Robots form the foundation of many of the systems covered in this review. Various form factors, from wearable exoskeletons to humanoid social robots, provide dynamic benefits, including physical assistance, real-time health monitoring, and haptic feedback. Visual interfaces, long overlooked, are now gaining prominence. With the proliferation of extended reality devices, richer and more immersive visual experiences are becoming available, benefiting HMI systems by providing detailed monitoring and feedback on user actions and statistics. Overall, highly integrated robotic systems leveraging biosignal feedback control and seamless data visualization are gaining traction among diverse user bases. These highly adaptable devices pave the way for further advancements in biotechnology, healthcare, and numerous other fields.

Author Declarations

The authors declare no conflict of interest at this time.

J. L., S. M., and A. B. contributed equally. J. L., S. M., and A. B. conducted the review, created figures, and wrote the paper. M.K., H.J., and W.Y. edited the manuscript.

Acknowledgements

We acknowledge the support of the National Science Foundation/the Centers for Disease Control and Prevention (grant NRI-2024742). W.-H.Y. acknowledges the support of the IEN Center Grant from the Georgia Tech Institute for Electronics and Nanotechnology.

References

[1] W. Dong *et al.*, "Soft human–machine interfaces: design, sensing and stimulation," *Int J Intell Robot Appl*, vol. 2, no. 3, pp. 313–338, Sep. 2018, doi: 10.1007/s41315-018-0060-z.

[2] G. Masengo, X. Zhang, R. Dong, A. B. Alhassan, K. Hamza, and E. Mudaheranwa, "Lower limb exoskeleton robot and its cooperative control: A review, trends, and challenges for future research," *Front Neurorobot*, vol. 16, Jan. 2023, doi: 10.3389/fnbot.2022.913748.

[3] W. Heng, S. Solomon, and W. Gao, "Flexible Electronics and Devices as Human–Machine Interfaces for Medical Robotics," *Advanced Materials*, vol. 34, no. 16, p. 2107902, Apr. 2022, doi: 10.1002/adma.202107902.

[4] R. A. Shaik and E. Rufus, "Recent trends and role of large area flexible electronics in shape sensing application – a review," *Industrial Robot: the international journal of robotics research and application*, vol. 48, no. 5, pp. 745–762, Sep. 2021, doi: 10.1108/IR-10-2020-0234.

[5] C. Appiah, C. Arndt, K. Siemsen, A. Heitmann, A. Staubitz, and C. Selhuber-Unkel, "Living Materials Herald a New Era in Soft Robotics," *Advanced Materials*, vol. 31, no. 36, p. 1807747, Sep. 2019, doi: 10.1002/adma.201807747.

[6] A. Gonzalez, L. Garcia, J. Kilby, and P. McNair, "Robotic devices for paediatric rehabilitation: a review of design features," *Biomed Eng Online*, vol. 20, no. 1, p. 89, Sep. 2021, doi: 10.1186/s12938-021-00920-5.

[7] M. AL-Quraishi, I. Elamvazuthi, S. Daud, S. Parasuraman, and A. Borboni, "EEG-Based Control for Upper and Lower Limb Exoskeletons and Prostheses: A Systematic Review," *Sensors*, vol. 18, no. 10, p. 3342, Oct. 2018, doi: 10.3390/s18103342.

[8] C. Zheng *et al.*, "Stretchable self-adhesive and self-powered smart bandage for motion perception and motion intention recognition," *Nano Energy*, vol. 109, p. 108245, May 2023, doi: 10.1016/j.nanoen.2023.108245.

[9] P. Li, Y. Meng, M. Li, X. Xuan, S. Xu, and H. Li, "An electroencephalography electrode based on a few-layer graphene/TiO2 nanotube nanoarchitecture for application in robot arm control," *Sens Actuators A Phys*, vol. 354, p. 114293, May 2023, doi: 10.1016/j.sna.2023.114293.

[10] S. Ramadurai, H. Jeong, and M. Kim, "Predicting the metabolic cost of exoskeleton-assisted squatting using foot pressure features and machine learning," *Front Robot AI*, vol. 10, Apr. 2023, doi: 10.3389/frobt.2023.1166248.

[11] H. Manjunatha, S. S. Jujjavarapu, and E. T. Esfahani, "Transfer Learning of Motor Difficulty Classification in Physical Human–Robot Interaction Using Electromyography," *J Comput Inf Sci Eng*, vol. 22, no. 5, Oct. 2022, doi: 10.1115/1.4054594.

[12] J. Kim *et al.*, "Soft wearable flexible bioelectronics integrated with an ankle-foot exoskeleton for estimation of metabolic costs and physical effort," *npj Flexible Electronics*, vol. 7, no. 1, p. 3, Jan. 2023, doi: 10.1038/s41528-023-00239-2.

[13] J. Kim *et al.*, "Mixed reality-integrated soft wearable biosensing glove for manipulating objects," *Biosens Bioelectron X*, vol. 14, p. 100343, Sep. 2023, doi: 10.1016/j.biosx.2023.100343.

[14] Y. Pang *et al.*, "Skin-inspired textile-based tactile sensors enable multifunctional sensing of wearables and soft robots," *Nano Energy*, vol. 96, p. 107137, Jun. 2022, doi: 10.1016/j.nanoen.2022.107137.

[15] J. Huang, G. Li, H. Su, and Z. Li, "Development and Continuous Control of an Intelligent Upper-Limb Neuroprosthesis for Reach and Grasp Motions Using Biological Signals," *IEEE Trans Syst Man Cybern Syst*, vol. 52, no. 6, pp. 3431–3441, Jun. 2022, doi: 10.1109/TSMC.2021.3069084.

[16] M. G. Antonelli, P. Beomonte Zobel, F. Durante, and M. Zeer, "Modeling-Based EMG Signal (MBES) Classifier for Robotic Remote-Control Purposes," *Actuators*, vol. 11, no. 3, p. 65, Feb. 2022, doi: 10.3390/act11030065.

[17] S. Duan, C. Wang, M. Li, Z. Su, J. Liu, and X. Wu, "A Framework for Human-Exoskeleton Interaction Based on sEMG Interface and Electrotactile Feedback," in *2021 IEEE International Conference on Real-time Computing and Robotics (RCAR)*, IEEE, Jul. 2021, pp. 269–274. doi: 10.1109/RCAR52367.2021.9517365.

[18] M. Kim *et al.*, "Visual guidance can help with the use of a robotic exoskeleton during human walking," *Sci Rep*, vol. 12, no. 1, p. 3881, Mar. 2022, doi: 10.1038/s41598-022-07736-w.

[19] P. Uluer, H. Kose, E. Gumuslu, and D. E. Barkana, "Experience with an Affective Robot Assistant for Children with Hearing Disabilities," *Int J Soc Robot*, vol. 15, no. 4, pp. 643–660, Apr. 2023, doi: 10.1007/s12369-021-00830-5.

[20] Y. Zhang, M. Bressel, S. De Groof, F. Domine, L. Labey, and L. Peyrodie, "Design and Control of a Size-Adjustable Pediatric Lower-Limb Exoskeleton Based on Weight Shift," *IEEE Access*, vol. 11, pp. 6372–6384, 2023, doi: 10.1109/ACCESS.2023.3235654.

[21] C. Mireles, M. Sanchez, D. Cruz-Ortiz, I. Salgado, and I. Chairez, "Home-care nursing controlled mobile robot with vital signal monitoring," *Med Biol Eng Comput*, vol. 61, no. 2, pp. 399–420, Feb. 2023, doi: 10.1007/s11517-022-02712-y.

[22] Y. Wu *et al.*, "Piezoresistive stretchable strain sensors with human machine interface demonstrations," *Sens Actuators A Phys*, vol. 279, pp. 46–52, Aug. 2018, doi: 10.1016/j.sna.2018.05.036.

[23] Y.-T. Kwon *et al.*, "All-printed nanomembrane wireless bioelectronics using a biocompatible solderable graphene for multimodal human-machine interfaces," *Nat Commun*, vol. 11, no. 1, p. 3450, Jul. 2020, doi: 10.1038/s41467-020-17288-0.

[24] H. Jeong, P. Haghighat, P. Kantharaju, M. Jacobson, H. Jeong, and M. Kim, "Muscle coordination and recruitment during squat assistance using a robotic ankle–foot exoskeleton," *Sci Rep*, vol. 13, no. 1, p. 1363, Jan. 2023, doi: 10.1038/s41598-023-28229-4.

[25] K. A. Witte, P. Fiers, A. L. Sheets-Singer, and S. H. Collins, "Improving the energy economy of human running with powered and unpowered ankle exoskeleton assistance," *Sci Robot*, vol. 5, no. 40, Mar. 2020, doi: 10.1126/scirobotics.aay9108.

[26] N. Seppich *et al.*, "CyberLimb: a novel robotic prosthesis concept with shared and intuitive control," *J Neuroeng Rehabil*, vol. 19, no. 1, p. 41, Dec. 2022, doi: 10.1186/s12984-022-01016-4.

[27] C. C. Cheah and X. Li, *Task-Space Sensory Feedback Control of Robot Manipulators*, vol. 73. in Intelligent Systems, Control and Automation: Science and Engineering, vol. 73. Singapore: Springer Singapore, 2015. doi: 10.1007/978-981-287-062-9.

[28] C. Mei, "On Teaching the Simplification of Block Diagrams," *International Journal of Engineering Education*, vol. 18, no. 6, pp. 697–703, 2002.

[29] X.-L. Yang *et al.*, "The history, hotspots, and trends of electrocardiogram," *Journal of Geriatric Cardiology*, vol. 12, no. 4, pp. 448–456, Jul. 2015.

[30] M. Kazamel and P. P. Warren, "History of electromyography and nerve conduction studies: A tribute to the founding fathers," *Journal of Clinical Neuroscience*, vol. 43, pp. 54–60, Sep. 2017, doi: 10.1016/j.jocn.2017.05.018.

[31] J. Koller, "'Body-in-the-Loop' Optimization of Assistive Robotic Devices: A Validation Study," *Robotics: Science and Systems*, vol. 2016, pp. 1–10, 2016.

[32] W. Felt, J. C. Selinger, J. M. Donelan, and C. D. Remy, "'Body-In-The-Loop': Optimizing Device Parameters Using Measures of Instantaneous Energetic Cost," *PLoS One*, vol. 10, no. 8, p. e0135342, Aug. 2015, doi: 10.1371/journal.pone.0135342.

[33] P. Kantharaju, H. Jeong, S. Ramadurai, M. Jacobson, H. Jeong, and M. Kim, "Reducing Squat Physical Effort Using Personalized Assistance From an Ankle Exoskeleton," *IEEE Transactions on Neural Systems and Rehabilitation Engineering*, vol. 30, pp. 1786–1795, 2022, doi: 10.1109/TNSRE.2022.3186692.

[34] D. S. Nunes, P. Zhang, and J. Sa Silva, "A Survey on Human-in-the-Loop Applications Towards an Internet of All," *IEEE Communications Surveys & Tutorials*, vol. 17, no. 2, pp. 944–965, Feb. 2015.

[35] P. Gergondet, D. Petit, and A. Kheddar, "Steering a robot with a brain-computer interface: Impact of video feedback on BCI performance," in *2012 IEEE RO-MAN: The 21st IEEE International Symposium on Robot and Human Interactive Communication*, IEEE, Sep. 2012, pp. 271–276. doi: 10.1109/ROMAN.2012.6343765.

[36] B. L. Fylstra, I.-C. Lee, M. Li, M. D. Lewek, and H. Huang, "Human-prosthesis cooperation: combining adaptive prosthesis control with visual feedback guided gait," *J Neuroeng Rehabil*, vol. 19, no. 1, p. 140, Dec. 2022, doi: 10.1186/s12984-022-01118-z.

[37] M. J. Page *et al.*, "The PRISMA 2020 statement: An updated guideline for reporting systematic reviews," *International Journal of Surgery*, vol. 88, p. 105906, Apr. 2021, doi: 10.1016/j.ijsu.2021.105906.

[38] Z. Leng *et al.*, "Sebum-Membrane-Inspired Protein-Based Bioprotonic Hydrogel for Artificial Skin and Human-Machine Merging Interface," *Adv Funct Mater*, vol. 33, no. 13, p. 2211056, Mar. 2023, doi: 10.1002/adfm.202211056.

[39] M. Zarei, G. Lee, S. G. Lee, and K. Cho, "Advances in Biodegradable Electronic Skin: Material Progress and Recent Applications in Sensing, Robotics, and Human–Machine Interfaces," *Advanced Materials*, vol. 35, no. 4, p. 2203193, Jan. 2023, doi: 10.1002/adma.202203193.

[40] M. Teplan, "Fundamentals of EEG measurement," *Measurement Science Review*, vol. 2, no. 2, 2002.

[41] P. Singh, S. D. Joshi, R. K. Patney, and K. Saha, "Fourier-Based Feature Extraction for Classification of EEG Signals Using EEG Rhythms," *Circuits Syst Signal Process*, vol. 35, no. 10, pp. 3700–3715, Oct. 2016, doi: 10.1007/s00034-015-0225-z.

[42] V. Kudva, R. B. Hegde, and C. Karimanasseri, "Use of Advanced Technology for Rehabilitation of Human Disabilities due to Damage to the CNS: A Review," *Crit Rev Phys Rehabil Med*, vol. 33, no. 1, pp. 43–65, 2021, doi: 10.1615/CritRevPhysRehabilMed.2021034999.

[43] M. Mahmood *et al.*, "VR-enabled portable brain-computer interfaces via wireless soft bioelectronics," *Biosens Bioelectron*, vol. 210, p. 114333, Aug. 2022, doi: 10.1016/j.bios.2022.114333.

[44] Q. Ai, M. Zhao, K. Chen, X. Zhao, L. Ma, and Q. Liu, "Flexible coding scheme for robotic arm control driven by motor imagery decoding," *J Neural Eng*, vol. 19, no. 5, p. 056008, Oct. 2022, doi: 10.1088/1741-2552/ac84a9.

[45] J. Cantillo-Negrete *et al.*, "Brain-Computer Interface Coupled to a Robotic Hand Orthosis for Stroke Patients' Neurorehabilitation: A Crossover Feasibility Study," *Front Hum Neurosci*, vol. 15, Jun. 2021, doi: 10.3389/fnhum.2021.656975.

[46] A. E. Hramov, V. A. Maksimenko, and A. N. Pisarchik, "Physical principles of brain–computer interfaces and their applications for rehabilitation, robotics and control of human brain states," *Phys Rep*, vol. 918, pp. 1–133, Jun. 2021, doi: 10.1016/j.physrep.2021.03.002.

[47] J. Tabbal, K. Mechref, and W. El-Falou, "Brain Computer Interface for smart living environment," in *2018 9th Cairo International Biomedical Engineering Conference (CIBEC)*, IEEE, Dec. 2018, pp. 61–64. doi: 10.1109/CIBEC.2018.8641827.

[48] Y. Song, S. Cai, L. Yang, G. Li, W. Wu, and L. Xie, "A Practical EEG-Based Human-Machine Interface to Online Control an Upper-Limb Assist Robot," *Front Neurorobot*, vol. 14, Jul. 2020, doi: 10.3389/fnbot.2020.00032.

[49] T. D. Lagerlund *et al.*, "Determination of 10–20 system electrode locations using magnetic resonance image scanning with markers," *Electroencephalogr Clin Neurophysiol*, vol. 86, no. 1, pp. 7–14, Jan. 1993, doi: 10.1016/0013-4694(93)90062-Z.

[50] X. Liang, Q. Zhao, and J. Liang, "Finger rehabilitation training and evaluation system based on EEG signals, machine learning and Fugl-Meyer scale," *J Phys Conf Ser*, vol. 2395, no. 1, p. 012060, Dec. 2022, doi: 10.1088/1742-6596/2395/1/012060.

[51] M. Mahmood *et al.*, "Fully portable and wireless universal brain–machine interfaces enabled by flexible scalp electronics and deep learning algorithm," *Nat Mach Intell*, vol. 1, no. 9, pp. 412–422, Sep. 2019, doi: 10.1038/s42256-019-0091-7.

[52] H. C. Siu, A. M. Arenas, T. Sun, and L. A. Stirling, "Implementation of a Surface Electromyography-Based Upper Extremity Exoskeleton Controller Using Learning from Demonstration," *Sensors*, vol. 18, no. 2, p. 467, Feb. 2018, doi: 10.3390/s18020467.

[53] L. Grazi, S. Crea, A. Parri, R. Molino Lova, S. Micera, and N. Vitiello, "Gastrocnemius Myoelectric Control of a Robotic Hip Exoskeleton Can Reduce the User's Lower-Limb Muscle Activities at Push Off," *Front Neurosci*, vol. 12, no. FEB, Feb. 2018, doi: 10.3389/fnins.2018.00071.

[54] P. A. Lopes, H. Paisana, A. T. De Almeida, C. Majidi, and M. Tavakoli, "Hydroprinted Electronics: Ultrathin Stretchable Ag–In–Ga E-Skin for Bioelectronics and Human–Machine Interaction," *ACS Appl Mater Interfaces*, vol. 10, no. 45, pp. 38760–38768, Nov. 2018, doi: 10.1021/acsami.8b13257.

[55] F. J. Badesa *et al.*, "Physiological Responses During Hybrid BNCI Control of an Upper-Limb Exoskeleton," *Sensors*, vol. 19, no. 22, p. 4931, Nov. 2019, doi: 10.3390/s19224931.

[56] L. E. Osborn *et al.*, "Prosthesis with neuromorphic multilayered e-dermis perceives touch and pain," *Sci Robot*, vol. 3, no. 19, Jun. 2018, doi: 10.1126/scirobotics.aat3818.

[57] E. Baka, A. Vishwanath, N. Mishra, G. Vleioras, and N. M. Thalmann, "'Am I Talking to a Human or a Robot?': A Preliminary Study of Human's Perception in Human-Humanoid Interaction and Its Effects in Cognitive and Emotional States," in *Lecture Notes in Computer Science (including subseries Lecture Notes in Artificial Intelligence and Lecture Notes in Bioinformatics)*, vol. 11542 LNCS, 2019, pp. 240–252. doi: 10.1007/978-3-030-22514-8_20.

[58] K. Miatliuk, A. Nawrocka, K. Holewa, and V. Moulianitis, "Conceptual Design of BCI for Mobile Robot Control," *Applied Sciences*, vol. 10, no. 7, p. 2557, Apr. 2020, doi: 10.3390/app10072557.

[59] F. Marini, J. Zenzeri, V. Pippo, P. Morasso, and C. Campus, "Neural correlates of proprioceptive upper limb position matching," *Hum Brain Mapp*, vol. 40, no. 16, pp. 4813–4826, Nov. 2019, doi: 10.1002/hbm.24739.

[60] P. Batres-Mendoza, E. I. Guerra-Hernandez, A. Espinal, E. Perez-Careta, and H. Rostro-Gonzalez, "Biologically-Inspired Legged Robot Locomotion Controlled With a BCI by Means of Cognitive Monitoring," *IEEE Access*, vol. 9, pp. 35766–35777, 2021, doi: 10.1109/ACCESS.2021.3062329.

[61] M. Staffa, M. Berardinelli, G. Acampora, M. Giordano, M. De Gregorio, and F. Ficuciello, "A Weightless Neural Network as a Classifier to Translate EEG Signals into Robotic hand Commands," in *2018 27th IEEE International Symposium on Robot and Human Interactive Communication (RO-MAN)*, IEEE, Aug. 2018, pp. 487–490. doi: 10.1109/ROMAN.2018.8525521.

[62] K.-J. Wang, H.-W. Tung, Z. Huang, P. Thakur, Z.-H. Mao, and M.-X. You, "EXGbuds," in *Companion of the 2018 ACM/IEEE International Conference on Human-Robot Interaction*, New York, NY, USA: ACM, Mar. 2018, pp. 369–370. doi: 10.1145/3173386.3177836.

[63] M. B. I. Reaz, M. S. Hussain, and F. Mohd-Yasin, "Techniques of EMG signal analysis: detection, processing, classification and applications," *Biol Proced Online*, vol. 8, no. 1, pp. 11–35, Dec. 2006, doi: 10.1251/bpo115.

[64] Y. Al-Ajam, A. Woollard, and N. Kang, "Advances in upper limb loss rehabilitation: the role of targeted muscle reinnervation and regenerative peripheral nerve interfaces," *Plast Aesthet Res*, vol. 9, p. 63, 2022, doi: 10.20517/2347-9264.2022.24.

[65] E. V Okorokova, Q. He, and S. J. Bensmaia, "Biomimetic encoding model for restoring touch in bionic hands through a nerve interface," *J Neural Eng*, vol. 15, no. 6, p. 066033, Dec. 2018, doi: 10.1088/1741-2552/aae398.

[66] E. P. Washabaugh, L. H. Cubillos, A. C. Nelson, B. T. Cargile, E. S. Claflin, and C. Krishnan, "Motor slacking during resisted treadmill walking: Can visual feedback of kinematics reduce this behavior?," *Gait Posture*, vol. 90, pp. 334–339, Oct. 2021, doi: 10.1016/j.gaitpost.2021.09.189.

[67] C. J. Hasson, "An Interactive Simulator for Imposing Virtual Musculoskeletal Dynamics," *IEEE Trans Biomed Eng*, vol. 65, no. 3, pp. 539–549, Mar. 2018, doi: 10.1109/TBME.2017.2703298.

[68] M. Kim, H. Lyness, T. Chen, and S. H. Collins, "The Effects of Prosthesis Inversion/Eversion Stiffness on Balance-Related Variability During Level Walking: A Pilot Study," *J Biomech Eng*, vol. 142, no. 9, Sep. 2020, doi: 10.1115/1.4046881.

[69] T.-C. Lin, A. U. Krishnan, and Z. Li, "Physical Fatigue Analysis of Assistive Robot Teleoperation via Whole-body Motion Mapping," in *2019 IEEE/RSJ International Conference on Intelligent Robots and Systems (IROS)*, IEEE, Nov. 2019, pp. 2240–2245. doi: 10.1109/IROS40897.2019.8968544.

[70] S. Cheon *et al.*, "Single EMG Sensor-Driven Robotic Glove Control for Reliable Augmentation of Power Grasping," *IEEE Trans Med Robot Bionics*, vol. 3, no. 1, pp. 179–189, Feb. 2021, doi: 10.1109/TMRB.2020.3046847.

[71] A. Krasoulis, S. Vijayakumar, and K. Nazarpour, "Effect of User Practice on Prosthetic Finger Control With an Intuitive Myoelectric Decoder," *Front Neurosci*, vol. 13, Sep. 2019, doi: 10.3389/fnins.2019.00891.

[72] R. G. Gaston, J. W. Bracey, M. A. Tait, and B. J. Loeffler, "A Novel Muscle Transfer for Independent Digital Control of a Myoelectric Prosthesis: The Starfish Procedure," *J Hand Surg Am*, vol. 44, no. 2, pp. 163.e1-163.e5, Feb. 2019, doi: 10.1016/j.jhsa.2018.04.009.

[73] E. Mastinu *et al.*, "Grip control and motor coordination with implanted and surface electrodes while grasping with an osseointegrated prosthetic hand," *J Neuroeng Rehabil*, vol. 16, no. 1, p. 49, Dec. 2019, doi: 10.1186/s12984-019-0511-2.

[74] A. Sturma, L. A. Hruby, A. Boesendorfer, C. Gstoettner, D. Farina, and O. C. Aszmann, "Therapy Interventions for Upper Limb Amputees Undergoing Selective Nerve Transfers," *Journal of Visualized Experiments*, no. 176, Oct. 2021, doi: 10.3791/62896.

[75] D. Blustein, A. Wilson, and J. Sensinger, "Assessing the quality of supplementary sensory feedback using the crossmodal congruency task," *Sci Rep*, vol. 8, no. 1, p. 6203, Apr. 2018, doi: 10.1038/s41598-018-24560-3.

[76] M. Hamaya *et al.*, "Exploiting Human and Robot Muscle Synergies for Human-in-the-loop Optimization of EMG-based Assistive Strategies," in *2019 International Conference on Robotics and Automation (ICRA)*, IEEE, May 2019, pp. 549–555. doi: 10.1109/ICRA.2019.8794082.

[77] K. Shi, R. Huang, Z. Peng, F. Mu, and X. Yang, "MCSNet: Channel Synergy-Based Human-Exoskeleton Interface With Surface Electromyogram," *Front Neurosci*, vol. 15, Nov. 2021, doi: 10.3389/fnins.2021.704603.

[78] F. Tamburella *et al.*, "Influences of the biofeedback content on robotic post-stroke gait rehabilitation: electromyographic vs joint torque biofeedback," *J Neuroeng Rehabil*, vol. 16, no. 1, p. 95, Dec. 2019, doi: 10.1186/s12984-019-0558-0.

[79] T. R. Clites *et al.*, "Proprioception from a neurally controlled lower-extremity prosthesis," *Sci Transl Med*, vol. 10, no. 443, May 2018, doi: 10.1126/scitranslmed.aap8373.

[80] S. Huang and H. Huang, "Voluntary Control of Residual Antagonistic Muscles in Transtibial Amputees: Feedforward Ballistic Contractions and Implications for Direct Neural Control of Powered Lower Limb Prostheses," *IEEE Transactions on Neural*

Systems and Rehabilitation Engineering, vol. 26, no. 4, pp. 894–903, Apr. 2018, doi: 10.1109/TNSRE.2018.2811544.

[81] O. N. Beck, M. K. Shepherd, R. Rastogi, G. Martino, L. H. Ting, and G. S. Sawicki, "Exoskeletons need to react faster than physiological responses to improve standing balance," *Sci Robot*, vol. 8, no. 75, Feb. 2023, doi: 10.1126/scirobotics.adf1080.

[82] W. Dong, C. Zhu, W. Hu, L. Xiao, and Y. Huang, "Stretchable human-machine interface based on skin-conformal sEMG electrodes with self-similar geometry," *Journal of Semiconductors*, vol. 39, no. 1, p. 014001, Jan. 2018, doi: 10.1088/1674-4926/39/1/014001.

[83] Y.-C. Lai *et al.*, "Actively Perceiving and Responsive Soft Robots Enabled by Self-Powered, Highly Extensible, and Highly Sensitive Triboelectric Proximity- and Pressure-Sensing Skins," *Advanced Materials*, vol. 30, no. 28, p. 1801114, Jul. 2018, doi: 10.1002/adma.201801114.

[84] A. L. Goldberger, Z. D. Goldberger, and A. Shvilkin, *Goldberger's Clinical Electrocardiography*, 9th ed. Elsevier, 2017. doi: 10.1016/C2014-0-03319-9.

[85] A. López and F. Ferrero, "Biomedical Signal Processing and Artificial Intelligence in EOG Signals," in *Advances in Non-Invasive Biomedical Signal Sensing and Processing with Machine Learning*, Cham: Springer International Publishing, 2023, pp. 185–206. doi: 10.1007/978-3-031-23239-8_8.

[86] S. Ban, Y. J. Lee, K. J. Yu, J. W. Chang, J.-H. Kim, and W.-H. Yeo, "Persistent Human–Machine Interfaces for Robotic Arm Control Via Gaze and Eye Direction Tracking," *Advanced Intelligent Systems*, vol. 5, no. 7, Jul. 2023, doi: 10.1002/aisy.202200408.

[87] C. Tan, F. Sun, B. Fang, T. Kong, and W. Zhang, "Autoencoder-based transfer learning in brain–computer interface for rehabilitation robot," *Int J Adv Robot Syst*, vol. 16, no. 2, p. 172988141984086, Mar. 2019, doi: 10.1177/1729881419840860.

[88] S. Ban *et al.*, "Soft Wireless Headband Bioelectronics and Electrooculography for Persistent Human–Machine Interfaces," *ACS Appl Electron Mater*, vol. 5, no. 2, pp. 877–886, Feb. 2023, doi: 10.1021/acsaelm.2c01436.

[89] S. Crea *et al.*, "Feasibility and safety of shared EEG/EOG and vision-guided autonomous whole-arm exoskeleton control to perform activities of daily living," *Sci Rep*, vol. 8, no. 1, p. 10823, Jul. 2018, doi: 10.1038/s41598-018-29091-5.

[90] M. Sharma, S. Kacker, and M. Sharma, "A Brief Introduction and Review on Galvanic Skin Response," *International Journal of Medical Research Professionals*, vol. 2, no. 6, Dec. 2016, doi: 10.21276/ijmrp.2016.2.6.003.

[91] J. Allen, "Photoplethysmography and its application in clinical physiological measurement," *Physiol Meas*, vol. 28, no. 3, pp. R1–R39, Mar. 2007, doi: 10.1088/0967-3334/28/3/R01.

[92] Y. Shi, N. Ruiz, R. Taib, E. Choi, and F. Chen, "Galvanic skin response (GSR) as an index of cognitive load," in *CHI '07 Extended Abstracts on Human Factors in Computing Systems*, New York, NY, USA: ACM, Apr. 2007, pp. 2651–2656. doi: 10.1145/1240866.1241057.

[93] Y. Hu, N. Abe, M. Benallegue, N. Yamanobe, G. Venture, and E. Yoshida, "Toward Active Physical Human–Robot Interaction: Quantifying the Human State During

Interactions," *IEEE Trans Hum Mach Syst*, vol. 52, no. 3, pp. 367–378, Jun. 2022, doi: 10.1109/THMS.2021.3138684.

[94] J. Fan, A. Ullal, L. Beuscher, L. C. Mion, P. Newhouse, and N. Sarkar, "Field Testing of Ro-Tri, a Robot-Mediated Triadic Interaction for Older Adults," *Int J Soc Robot*, vol. 13, no. 7, pp. 1711–1727, Nov. 2021, doi: 10.1007/s12369-021-00760-2.

[95] R. Agrigoroaie and A. Tapus, "Physiological Parameters Variation Based on the Sensory Stimuli used by a Robot in a News Reading Task," in *2018 27th IEEE International Symposium on Robot and Human Interactive Communication (RO-MAN)*, IEEE, Aug. 2018, pp. 618–625. doi: 10.1109/ROMAN.2018.8525766.

[96] O. Rudovic, J. Lee, M. Dai, B. Schuller, and R. W. Picard, "Personalized machine learning for robot perception of affect and engagement in autism therapy," *Sci Robot*, vol. 3, no. 19, Jun. 2018, doi: 10.1126/scirobotics.aao6760.

[97] L. Peternel and A. Ajoudani, "After a Decade of Teleimpedance: A Survey," *IEEE Trans Hum Mach Syst*, vol. 53, no. 2, pp. 401–416, Apr. 2023, doi: 10.1109/THMS.2022.3231703.

[98] T. Seel, J. Raisch, and T. Schauer, "IMU-Based Joint Angle Measurement for Gait Analysis," *Sensors*, vol. 14, no. 4, pp. 6891–6909, Apr. 2014, doi: 10.3390/s140406891.

[99] I. E. Jaramillo *et al.*, "Real-Time Human Activity Recognition with IMU and Encoder Sensors in Wearable Exoskeleton Robot via Deep Learning Networks," *Sensors*, vol. 22, no. 24, p. 9690, Dec. 2022, doi: 10.3390/s22249690.

[100] A. T. Asbeck, S. M. M. De Rossi, I. Galiana, Y. Ding, and C. J. Walsh, "Stronger, Smarter, Softer: Next-Generation Wearable Robots," *IEEE Robot Autom Mag*, vol. 21, no. 4, pp. 22–33, Dec. 2014, doi: 10.1109/MRA.2014.2360283.

[101] J. Sun, Y. Shen, and J. Rosen, "Sensor Reduction, Estimation, and Control of an Upper-Limb Exoskeleton," *IEEE Robot Autom Lett*, vol. 6, no. 2, pp. 1012–1019, Apr. 2021, doi: 10.1109/LRA.2021.3056366.

[102] M. O. Ibitoye, N. A. Hamzaid, J. M. Zuniga, and A. K. Abdul Wahab, "Mechanomyography and muscle function assessment: A review of current state and prospects," *Clinical Biomechanics*, vol. 29, no. 6, pp. 691–704, Jun. 2014, doi: 10.1016/j.clinbiomech.2014.04.003.

[103] S. Wilson *et al.*, "Formulation of a new gradient descent MARG orientation algorithm: Case study on robot teleoperation," *Mech Syst Signal Process*, vol. 130, pp. 183–200, Sep. 2019, doi: 10.1016/j.ymssp.2019.04.064.

[104] B. Stephens-Fripp, G. Alici, and R. Mutlu, "A Review of Non-Invasive Sensory Feedback Methods for Transradial Prosthetic Hands," *IEEE Access*, vol. 6, pp. 6878–6899, 2018, doi: 10.1109/ACCESS.2018.2791583.

[105] H. A. Haugen, L. Chan, and F. Li, "Indirect Calorimetry: A Practical Guide for Clinicians," *Nutrition in Clinical Practice*, vol. 22, no. 4, pp. 377–388, Aug. 2007, doi: 10.1177/0115426507022004377.

[106] M. Jacobson *et al.*, "Foot contact forces can be used to personalize a wearable robot during human walking," *Sci Rep*, vol. 12, no. 1, p. 10947, Jun. 2022, doi: 10.1038/s41598-022-14776-9.

[107] T.-C. Wen, M. Jacobson, X. Zhou, H.-J. Chung, and M. Kim, "The personalization of stiffness for an ankle-foot prosthesis emulator using Human-in-the-loop optimization," in

2020 IEEE/RSJ International Conference on Intelligent Robots and Systems (IROS), IEEE, Oct. 2020, pp. 3431–3436. doi: 10.1109/IROS45743.2020.9341101.

[108] D. C. Simonson and R. A. DeFronzo, "Indirect calorimetry: methodological and interpretative problems," *American Journal of Physiology-Endocrinology and Metabolism*, vol. 258, no. 3, pp. E399–E412, Mar. 1990, doi: 10.1152/ajpendo.1990.258.3.E399.

[109] I. Kang, H. Hsu, and A. Young, "The Effect of Hip Assistance Levels on Human Energetic Cost Using Robotic Hip Exoskeletons," *IEEE Robot Autom Lett*, vol. 4, no. 2, pp. 430–437, Apr. 2019, doi: 10.1109/LRA.2019.2890896.

[110] X. Zhao, Y. Ma, J. Huang, J. Zheng, and Y. Dong, "An Adaptive Real-time Gesture Detection Method Using EMG and IMU Series for Robot Control," in *2021 IEEE International Conference on Unmanned Systems (ICUS)*, IEEE, Oct. 2021, pp. 539–547. doi: 10.1109/ICUS52573.2021.9641278.

[111] R. Dindorf and P. Wos, "Using the Bioelectric Signals to Control of Wearable Orthosis of the Elbow Joint with Bi-Muscular Pneumatic Servo-Drive," *Robotica*, vol. 38, no. 5, pp. 804–818, May 2020, doi: 10.1017/S0263574719001097.

[112] L. Zhang *et al.*, "Fully organic compliant dry electrodes self-adhesive to skin for long-term motion-robust epidermal biopotential monitoring," *Nat Commun*, vol. 11, no. 1, p. 4683, Sep. 2020, doi: 10.1038/s41467-020-18503-8.

[113] L. Tian *et al.*, "Large-area MRI-compatible epidermal electronic interfaces for prosthetic control and cognitive monitoring," *Nat Biomed Eng*, vol. 3, no. 3, pp. 194–205, Feb. 2019, doi: 10.1038/s41551-019-0347-x.

[114] H. Jeong, Y. Noh, S. H. Ko, and D. Lee, "Flexible resistive pressure sensor with silver nanowire networks embedded in polymer using natural formation of air gap," *Compos Sci Technol*, vol. 174, pp. 50–57, Apr. 2019, doi: 10.1016/j.compscitech.2019.01.028.

[115] K. K. Kim *et al.*, "Highly Sensitive and Stretchable Multidimensional Strain Sensor with Prestrained Anisotropic Metal Nanowire Percolation Networks," *Nano Lett*, vol. 15, no. 8, pp. 5240–5247, Aug. 2015, doi: 10.1021/acs.nanolett.5b01505.

[116] L. Wang, X. Gao, L. Jin, Q. Wu, Z. Chen, and X. Lin, "Amperometric glucose biosensor based on silver nanowires and glucose oxidase," *Sens Actuators B Chem*, vol. 176, pp. 9–14, Jan. 2013, doi: 10.1016/j.snb.2012.08.077.

[117] I. Hong *et al.*, "Semipermanent Copper Nanowire Network with an Oxidation-Proof Encapsulation Layer," *Adv Mater Technol*, vol. 4, no. 4, Apr. 2019, doi: 10.1002/admt.201800422.

[118] I. Hong *et al.*, "Study on the oxidation of copper nanowire network electrodes for skin mountable flexible, stretchable and wearable electronics applications," *Nanotechnology*, vol. 30, no. 7, p. 074001, Feb. 2019, doi: 10.1088/1361-6528/aaf35c.

[119] D. Kim *et al.*, "Biocompatible Cost-Effective Electrophysiological Monitoring with Oxidation-Free Cu–Au Core–Shell Nanowire," *Adv Mater Technol*, vol. 5, no. 12, Dec. 2020, doi: 10.1002/admt.202000661.

[120] D. Kim *et al.*, "A Transparent and Flexible Capacitive-Force Touch Pad from High-Aspect-Ratio Copper Nanowires with Enhanced Oxidation Resistance for Applications in Wearable Electronics," *Small Methods*, vol. 2, no. 7, Jul. 2018, doi: 10.1002/smtd.201800077.

[121] J. Bang, Y. Jung, H. Kim, D. Kim, M. Cho, and S. H. Ko, "Multi-Bandgap Monolithic Metal Nanowire Percolation Network Sensor Integration by Reversible Selective Laser-Induced Redox," *Nanomicro Lett*, vol. 14, no. 1, p. 49, Dec. 2022, doi: 10.1007/s40820-021-00786-1.

[122] P. Zhan *et al.*, "A fibrous flexible strain sensor with Ag nanoparticles and carbon nanotubes for synergetic high sensitivity and large response range," *Compos Part A Appl Sci Manuf*, vol. 167, p. 107431, Apr. 2023, doi: 10.1016/j.compositesa.2023.107431.

[123] Y.-J. Tsai *et al.*, "Multilayered Ag NP–PEDOT–Paper Composite Device for Human–Machine Interfacing," *ACS Appl Mater Interfaces*, vol. 11, no. 10, pp. 10380–10388, Mar. 2019, doi: 10.1021/acsami.8b21390.

[124] K. K. Kim, J. Choi, J. Kim, S. Nam, and S. H. Ko, "Evolvable Skin Electronics by In Situ and In Operando Adaptation," *Adv Funct Mater*, vol. 32, no. 4, Jan. 2022, doi: 10.1002/adfm.202106329.

[125] J. Shin *et al.*, "Sensitive Wearable Temperature Sensor with Seamless Monolithic Integration," *Advanced Materials*, vol. 32, no. 2, Jan. 2020, doi: 10.1002/adma.201905527.

[126] D. Won *et al.*, "Transparent Electronics for Wearable Electronics Application," *Chem Rev*, vol. 123, no. 16, pp. 9982–10078, Aug. 2023, doi: 10.1021/acs.chemrev.3c00139.

[127] P. Won *et al.*, "Transparent Soft Actuators/Sensors and Camouflage Skins for Imperceptible Soft Robotics," *Advanced Materials*, vol. 33, no. 19, May 2021, doi: 10.1002/adma.202002397.

[128] P. Won *et al.*, "Stretchable and Transparent Kirigami Conductor of Nanowire Percolation Network for Electronic Skin Applications," *Nano Lett*, vol. 19, no. 9, pp. 6087–6096, Sep. 2019, doi: 10.1021/acs.nanolett.9b02014.

[129] J. Chen, G. Zhu, J. Wang, X. Chang, and Y. Zhu, "Multifunctional Iontronic Sensor Based on Liquid Metal-Filled Ho llow Ionogel Fibers in Detecting Pressure, Temperature, and Proximity," *ACS Appl Mater Interfaces*, vol. 15, no. 5, pp. 7485–7495, Feb. 2023, doi: 10.1021/acsami.2c22835.

[130] M. Wang *et al.*, "Fusing Stretchable Sensing Technology with Machine Learning for Human–Machine Interfaces," *Adv Funct Mater*, vol. 31, no. 39, Sep. 2021, doi: 10.1002/adfm.202008807.

[131] K. K. Kim *et al.*, "A substrate-less nanomesh receptor with meta-learning for rapid hand task recognition," *Nat Electron*, Dec. 2022, doi: 10.1038/s41928-022-00888-7.

[132] K. K. Kim *et al.*, "A deep-learned skin sensor decoding the epicentral human motions," *Nat Commun*, vol. 11, no. 1, p. 2149, May 2020, doi: 10.1038/s41467-020-16040-y.

[133] Y.-T. Kwon, H. Kim, M. Mahmood, Y.-S. Kim, C. Demolder, and W.-H. Yeo, "Printed, Wireless, Soft Bioelectronics and Deep Learning Algorithm for Smart Human–Machine Interfaces," *ACS Appl Mater Interfaces*, vol. 12, no. 44, pp. 49398–49406, Nov. 2020, doi: 10.1021/acsami.0c14193.

[134] B. Nicholls *et al.*, "An EMG-based Eating Behaviour Monitoring system with haptic feedback to promote mindful eating," *Comput Biol Med*, vol. 149, p. 106068, Oct. 2022, doi: 10.1016/j.compbiomed.2022.106068.

[135] A. Buerkle, W. Eaton, N. Lohse, T. Bamber, and P. Ferreira, "EEG based arm movement intention recognition towards enhanced safety in symbiotic Human-Robot Collaboration,"

Robot Comput Integr Manuf, vol. 70, p. 102137, Aug. 2021, doi: 10.1016/j.rcim.2021.102137.

[136] D. Kortenkamp, E. Huber, and R. Bonasso, "Recognizing and interpreting gestures on a mobile robot," in *Proceedings of the National Conference on Artificial Intelligence*, Citeseer, 1996.

[137] J. Winkler and M. Beetz, "Robot action plans that form and maintain expectations," in *2015 IEEE/RSJ International Conference on Intelligent Robots and Systems (IROS)*, IEEE, Sep. 2015, pp. 5174–5180. doi: 10.1109/IROS.2015.7354106.

[138] J. Arents and M. Greitans, "Smart Industrial Robot Control Trends, Challenges and Opportunities within Manufacturing," *Applied Sciences*, vol. 12, no. 2, p. 937, Jan. 2022, doi: 10.3390/app12020937.

[139] Y. Guo *et al.*, "Development Status and Multilevel Classification Strategy of Medical Robots," *Electronics (Basel)*, vol. 10, no. 11, p. 1278, May 2021, doi: 10.3390/electronics10111278.

[140] M. Kyrarini *et al.*, "A Survey of Robots in Healthcare," *Technologies (Basel)*, vol. 9, no. 1, p. 8, Jan. 2021, doi: 10.3390/technologies9010008.

[141] N. Sultan, "Reflective thoughts on the potential and challenges of wearable technology for healthcare provision and medical education," *Int J Inf Manage*, vol. 35, no. 5, pp. 521–526, Oct. 2015, doi: 10.1016/j.ijinfomgt.2015.04.010.

[142] T. L. Chen *et al.*, "Robots for humanity: using assistive robotics to empower people with disabilities," *IEEE Robot Autom Mag*, vol. 20, no. 1, pp. 30–39, Mar. 2013, doi: 10.1109/MRA.2012.2229950.

[143] I. Sanz-Pena, H. Jeong, and M. Kim, "Personalized Wearable Ankle Robot Using Modular Additive Manufacturing Design," *IEEE Robot Autom Lett*, vol. 8, no. 8, pp. 4935–4942, Aug. 2023, doi: 10.1109/LRA.2023.3290529.

[144] M. Belas dos Santos, C. Barros de Oliveira, A. dos Santos, C. Garabello Pires, V. Dylewski, and R. M. Arida, "A Comparative Study of Conventional Physiotherapy versus Robot-Assisted Gait Training Associated to Physiotherapy in Individuals with Ataxia after Stroke," *Behavioural Neurology*, vol. 2018, pp. 1–6, 2018, doi: 10.1155/2018/2892065.

[145] P. Geethanjali, "Myoelectric control of prosthetic hands: state-of-the-art review," *Medical Devices: Evidence and Research*, vol. Volume 9, pp. 247–255, Jul. 2016, doi: 10.2147/MDER.S91102.

[146] A. Lerner and M. Soudry, *Armed Conflict Injuries to the Extremities: A Treatment Manual*. Springer Science & Business Media, 2011.

[147] S. M. O'Connor and A. D. Kuo, "Direction-Dependent Control of Balance During Walking and Standing," *J Neurophysiol*, vol. 102, no. 3, pp. 1411–1419, Sep. 2009, doi: 10.1152/jn.00131.2009.

[148] M. Kim and S. H. Collins, "Step-to-Step Ankle Inversion/Eversion Torque Modulation Can Reduce Effort Associated with Balance," *Front Neurorobot*, vol. 11, Nov. 2017, doi: 10.3389/fnbot.2017.00062.

[149] T. Vandemeulebroucke, B. Dierckx de Casterlé, and C. Gastmans, "The use of care robots in aged care: A systematic review of argument-based ethics literature," *Arch Gerontol Geriatr*, vol. 74, pp. 15–25, Jan. 2018, doi: 10.1016/j.archger.2017.08.014.

[150] R. Hashim and H. Yussof, "Feasibility of care robots for children with special needs: A review," in *2017 IEEE International Symposium on Robotics and Intelligent Sensors (IRIS)*, IEEE, Oct. 2017, pp. 379–382. doi: 10.1109/IRIS.2017.8250152.

[151] V. N. Vahia, "Diagnostic and statistical manual of mental disorders 5: A quick glance," *Indian J Psychiatry*, vol. 55, no. 3, pp. 220–223, 2013.

[152] R. Sorbello *et al.*, "A Human–Humanoid Interaction Through the Use of BCI for Locked-In ALS Patients Using Neuro-Biological Feedback Fusion," *IEEE Transactions on Neural Systems and Rehabilitation Engineering*, vol. 26, no. 2, pp. 487–497, Feb. 2018, doi: 10.1109/TNSRE.2017.2728140.

[153] R. Zhang *et al.*, "Control of a Wheelchair in an Indoor Environment Based on a Brain–Computer Interface and Automated Navigation," *IEEE Transactions on Neural Systems and Rehabilitation Engineering*, vol. 24, no. 1, pp. 128–139, Jan. 2016, doi: 10.1109/TNSRE.2015.2439298.

[154] G. Lange, C. Y. Low, K. Johar, F. A. Hanapiah, and F. Kamaruzaman, "Classification of Electroencephalogram Data from Hand Grasp and Release Movements for BCI Controlled Prosthesis," *Procedia Technology*, vol. 26, pp. 374–381, 2016, doi: 10.1016/j.protcy.2016.08.048.

[155] Q. Huang, Z. Zhang, T. Yu, S. He, and Y. Li, "An EEG-/EOG-Based Hybrid Brain-Computer Interface: Application on Controlling an Integrated Wheelchair Robotic Arm System," *Front Neurosci*, vol. 13, Nov. 2019, doi: 10.3389/fnins.2019.01243.

[156] H. Zhu *et al.*, "IMU Motion Capture Method with Adaptive Tremor Attenuation in Teleoperation Robot System," *Sensors*, vol. 22, no. 9, p. 3353, Apr. 2022, doi: 10.3390/s22093353.

[157] C. Savur, S. Kumar, and F. Sahin, "A Framework for Monitoring Human Physiological Response during Human Robot Collaborative Task," in *2019 IEEE International Conference on Systems, Man and Cybernetics (SMC)*, IEEE, Oct. 2019, pp. 385–390. doi: 10.1109/SMC.2019.8914593.

[158] E. Zheng, Y. Li, Z. Zhao, Q. Wang, and H. Qiao, "An Electrical Impedance Tomography Based Interface for Human-Robot Collaboration," *IEEE/ASME Transactions on Mechatronics*, vol. 26, no. 5, pp. 2373–2384, 2021, doi: 10.1109/TMECH.2020.3039017.

[159] P. Li and X. Liu, "Common Sensors in Industrial Robots: A Review," *J Phys Conf Ser*, vol. 1267, no. 1, p. 012036, Jul. 2019, doi: 10.1088/1742-6596/1267/1/012036.

[160] C. W. Nielsen, M. A. Goodrich, and R. W. Ricks, "Ecological Interfaces for Improving Mobile Robot Teleoperation," *IEEE Transactions on Robotics*, vol. 23, no. 5, pp. 927–941, Oct. 2007, doi: 10.1109/TRO.2007.907479.

[161] J. Cui, S. Tosunoglu, R. Roberts, C. Moore, and D. W. Repperger, "A REVIEW OF TELEOPERATION SYSTEM CONTROL."

[162] P. C. Leger *et al.*, "Mars Exploration Rover Surface Operations: Driving Spirit at Gusev Crater," in *2005 IEEE International Conference on Systems, Man and Cybernetics*, IEEE, pp. 1815–1822. doi: 10.1109/ICSMC.2005.1571411.

[163] P. Wells and D. Deguire, "TALON: a universal unmanned ground vehicle platform, enabling the mission to be the focus," G. R. Gerhart, C. M. Shoemaker, and D. W. Gage, Eds., May 2005, p. 747. doi: 10.1117/12.602887.

[164] E. I. Agba, "SeaMaster: an ROV-manipulator system simulator," *IEEE Comput Graph Appl*, vol. 15, no. 1, pp. 24–31, 1995, doi: 10.1109/38.364959.
[165] P. Milgram and J. Ballantyne, "Real world teleoperation via virtual environment modeling," in *International Conference on Artificial Reality & Tele-existence ICAT'97*, Tokyo, 1997.
[166] J. Albiez, M. Hildebrand, T. Vogele, S. Joyeux, and F. Kirchner, "Robust Robots for Arctic Exploration," in *All Days*, OTC, Feb. 2011. doi: 10.4043/22120-MS.
[167] D. McLeod, "Emerging capabilities for autonomous inspection repair and maintenance," in *OCEANS 2010 MTS/IEEE SEATTLE*, IEEE, Sep. 2010, pp. 1–4. doi: 10.1109/OCEANS.2010.5664441.
[168] A. Shukla and H. Karki, "Application of robotics in onshore oil and gas industry—A review Part I," *Rob Auton Syst*, vol. 75, pp. 490–507, Jan. 2016, doi: 10.1016/j.robot.2015.09.012.
[169] C. Yang, J. Chen, Z. Li, W. He, and C.-Y. Su, "Development of a physiological signals enhanced teleoperation strategy," in *2015 IEEE International Conference on Information and Automation*, IEEE, Aug. 2015, pp. 13–19. doi: 10.1109/ICInfA.2015.7279251.
[170] K. Chandan, V. Kudalkar, X. Li, and S. Zhang, "ARROCH: Augmented Reality for Robots Collaborating with a Human," in *2021 IEEE International Conference on Robotics and Automation (ICRA)*, IEEE, May 2021, pp. 3787–3793. doi: 10.1109/ICRA48506.2021.9561144.
[171] K.-J. Wang, C. Y. Zheng, and Z.-H. Mao, "Human-Centered, Ergonomic Wearable Device with Computer Vision Augmented Intelligence for VR Multimodal Human-Smart Home Object Interaction," in *2019 14th ACM/IEEE International Conference on Human-Robot Interaction (HRI)*, IEEE, Mar. 2019, pp. 767–768. doi: 10.1109/HRI.2019.8673156.
[172] T. Teramae, K. Ishihara, J. Babič, J. Morimoto, and E. Oztop, "Human-In-The-Loop Control and Task Learning for Pneumatically Actuated Muscle Based Robots," *Front Neurorobot*, vol. 12, no. November, Nov. 2018, doi: 10.3389/fnbot.2018.00071.
[173] A. C. Simões, A. Pinto, J. Santos, S. Pinheiro, and D. Romero, "Designing human-robot collaboration (HRC) workspaces in industrial settings: A systematic literature review," *J Manuf Syst*, vol. 62, pp. 28–43, Jan. 2022, doi: 10.1016/j.jmsy.2021.11.007.
[174] S. Proia, R. Carli, G. Cavone, and M. Dotoli, "A Literature Review on Control Techniques for Collaborative Robotics in Industrial Applications," in *2021 IEEE 17th International Conference on Automation Science and Engineering (CASE)*, IEEE, Aug. 2021, pp. 591–596. doi: 10.1109/CASE49439.2021.9551600.
[175] S. Ramadurai and H. Jeong, "Effect of Human Involvement on Work Performance and Fluency in Human-Robot Collaboration for Recycling," in *2022 17th ACM/IEEE International Conference on Human-Robot Interaction (HRI)*, IEEE, Mar. 2022, pp. 1007–1011. doi: 10.1109/HRI53351.2022.9889606.
[176] V. Villani, F. Pini, F. Leali, and C. Secchi, "Survey on human–robot collaboration in industrial settings: Safety, intuitive interfaces and applications," *Mechatronics*, vol. 55, pp. 248–266, Nov. 2018, doi: 10.1016/j.mechatronics.2018.02.009.
[177] K.-B. Park, S. H. Choi, J. Y. Lee, Y. Ghasemi, M. Mohammed, and H. Jeong, "Hands-Free Human–Robot Interaction Using Multimodal Gestures and Deep Learning in Wearable Mixed Reality," *IEEE Access*, vol. 9, pp. 55448–55464, 2021, doi: 10.1109/ACCESS.2021.3071364.

[178] W. Li, Y. Hu, Y. Zhou, and D. T. Pham, "Safe human–robot collaboration for industrial settings: a survey," *J Intell Manuf*, Jun. 2023, doi: 10.1007/s10845-023-02159-4.
[179] S. H. Choi *et al.*, "An integrated mixed reality system for safety-aware human-robot collaboration using deep learning and digital twin generation," *Robot Comput Integr Manuf*, vol. 73, p. 102258, Feb. 2022, doi: 10.1016/j.rcim.2021.102258.
[180] R. N. Roy, N. Drougard, T. Gateau, F. Dehais, and C. P. C. Chanel, "How Can Physiological Computing Benefit Human-Robot Interaction?," *Robotics*, vol. 9, no. 4, p. 100, Nov. 2020, doi: 10.3390/robotics9040100.
[181] T. Williams, D. Szafir, T. Chakraborti, and H. Ben Amor, "Virtual, Augmented, and Mixed Reality for Human-Robot Interaction," in *Companion of the 2018 ACM/IEEE International Conference on Human-Robot Interaction*, New York, NY, USA: ACM, Mar. 2018, pp. 403–404. doi: 10.1145/3173386.3173561.
[182] S. Kumar and F. Sahin, "A framework for an adaptive human-robot collaboration approach through perception-based real-time adjustments of robot behavior in industry," in *2017 12th System of Systems Engineering Conference (SoSE)*, IEEE, Jun. 2017, pp. 1–6. doi: 10.1109/SYSOSE.2017.7994967.
[183] F. Pistolesi and B. Lazzerini, "Assessing the Risk of Low Back Pain and Injury via Inertial and Barometric Sensors," *IEEE Trans Industr Inform*, vol. 16, no. 11, pp. 7199–7208, Nov. 2020, doi: 10.1109/TII.2020.2992984.
[184] O. Flor-Unda, B. Casa, M. Fuentes, S. Solorzano, F. Narvaez-Espinoza, and P. Acosta-Vargas, "Exoskeletons: Contribution to Occupational Health and Safety," *Bioengineering*, vol. 10, no. 9, p. 1039, Sep. 2023, doi: 10.3390/bioengineering10091039.
[185] D. Romero, S. Mattsson, Å. Fast-Berglund, T. Wuest, D. Gorecky, and J. Stahre, "Digitalizing Occupational Health, Safety and Productivity for the Operator 4.0," 2018, pp. 473–481. doi: 10.1007/978-3-319-99707-0_59.
[186] G. Saridis, "Intelligent robotic control," *IEEE Trans Automat Contr*, vol. 28, no. 5, pp. 547–557, May 1983, doi: 10.1109/TAC.1983.1103278.
[187] M. R. Tucker *et al.*, "Control strategies for active lower extremity prosthetics and orthotics: a review," *J Neuroeng Rehabil*, vol. 12, no. 1, p. 1, 2015, doi: 10.1186/1743-0003-12-1.
[188] D. Nakhaeinia, S. Tang, S. Mohd Noor, and O. Motlagh, "A review of control architectures for autonomous navigation of mobile robots ," *International Journal of the Physical Sciences* , vol. Vol. 6, no. 2, pp. 169–174, Jan. 2011.
[189] M. A. Diaz *et al.*, "Human-in-the-Loop Optimization of Wearable Robotic Devices to Improve Human–Robot Interaction: A Systematic Review," *IEEE Trans Cybern*, pp. 1–14, 2022, doi: 10.1109/TCYB.2022.3224895.
[190] R. Baud, A. R. Manzoori, A. Ijspeert, and M. Bouri, "Review of control strategies for lower-limb exoskeletons to assist gait," *J Neuroeng Rehabil*, vol. 18, no. 1, p. 119, Dec. 2021, doi: 10.1186/s12984-021-00906-3.
[191] G. Li, Z. Li, J. Li, Y. Liu, and H. Qiao, "Muscle-Synergy-Based Planning and Neural-Adaptive Control for a Prosthetic Arm," *IEEE Transactions on Artificial Intelligence*, vol. 2, no. 5, pp. 424–436, Oct. 2021, doi: 10.1109/TAI.2021.3091038.
[192] N. Robinson, R. Mane, T. Chouhan, and C. Guan, "Emerging trends in BCI-robotics for motor control and rehabilitation," *Curr Opin Biomed Eng*, vol. 20, p. 100354, Dec. 2021, doi: 10.1016/j.cobme.2021.100354.

[193] V. Jusas and S. G. Samuvel, "Classification of Motor Imagery Using Combination of Feature Extraction and Reduction Methods for Brain-Computer Interface," *Information Technology And Control*, vol. 48, no. 2, pp. 225–234, Jun. 2019, doi: 10.5755/j01.itc.48.2.23091.

[194] W. Li *et al.*, "Preliminary study of online real-time control system for lower extremity exoskeletons based on EEG and sEMG fusion," in *2022 IEEE International Conference on Robotics and Biomimetics (ROBIO)*, IEEE, Dec. 2022, pp. 1689–1694. doi: 10.1109/ROBIO55434.2022.10011813.

[195] N. Kashiri *et al.*, "An Overview on Principles for Energy Efficient Robot Locomotion," *Front Robot AI*, vol. 5, Dec. 2018, doi: 10.3389/frobt.2018.00129.

[196] G. S. Sawicki, O. N. Beck, I. Kang, and A. J. Young, "The exoskeleton expansion: improving walking and running economy," *J Neuroeng Rehabil*, vol. 17, no. 1, p. 25, Dec. 2020, doi: 10.1186/s12984-020-00663-9.

[197] P. Kantharaju and M. Kim, "Phase-Plane Based Model-Free Estimation of Steady-State Metabolic Cost," *IEEE Access*, vol. 10, pp. 97642–97650, 2022, doi: 10.1109/ACCESS.2022.3205629.

[198] M. Kim *et al.*, "Bayesian Optimization of Soft Exosuits Using a Metabolic Estimator Stopping Process," in *2019 International Conference on Robotics and Automation (ICRA)*, IEEE, May 2019, pp. 9173–9179. doi: 10.1109/ICRA.2019.8793817.

[199] R. Di Marco *et al.*, "Experimental Protocol to Assess Neuromuscular Plasticity Induced by an Exoskeleton Training Session," *Methods Protoc*, vol. 4, no. 3, p. 48, Jul. 2021, doi: 10.3390/mps4030048.

[200] M. Gandolla, E. Guanziroli, A. D'Angelo, G. Cannaviello, F. Molteni, and A. Pedrocchi, "Automatic Setting Procedure for Exoskeleton-Assisted Overground Gait: Proof of Concept on Stroke Population," *Front Neurorobot*, vol. 12, no. MAR, Mar. 2018, doi: 10.3389/fnbot.2018.00010.

[201] T. Luth, D. Ojdanic, O. Friman, O. Prenzel, and A. Graser, "Low level control in a semi-autonomous rehabilitation robotic system via a Brain-Computer Interface," in *2007 IEEE 10th International Conference on Rehabilitation Robotics*, IEEE, Jun. 2007, pp. 721–728. doi: 10.1109/ICORR.2007.4428505.

[202] A. Nasr, A. Hashemi, and J. McPhee, "Model-Based Mid-Level Regulation for Assist-As-Needed Hierarchical Control of Wearable Robots: A Computational Study of Human-Robot Adaptation," *Robotics*, vol. 11, no. 1, p. 20, Jan. 2022, doi: 10.3390/robotics11010020.

[203] H. F. N. Al-Shuka, M. H. Rahman, S. Leonhardt, I. Ciobanu, and M. Berteanu, "Biomechanics, actuation, and multi-level control strategies of power-augmentation lower extremity exoskeletons: an overview," *Int J Dyn Control*, vol. 7, no. 4, pp. 1462–1488, Dec. 2019, doi: 10.1007/s40435-019-00517-w.

[204] J. Y. S. Luh, "Conventional controller design for industrial robots — A tutorial," *IEEE Trans Syst Man Cybern*, vol. SMC-13, no. 3, pp. 298–316, May 1983, doi: 10.1109/TSMC.1983.6313163.

[205] M. Ghandi, "Cyber-Physical Emotive Spaces: Human Cyborg, Data, and Biofeedback Emotive Interaction with Compassionate Spaces," in *Blucher Design Proceedings*, São

Paulo: Editora Blucher, Dec. 2019, pp. 655–664. doi: 10.5151/proceedings-ecaadesigradi2019_200.

[206] G. A. Pratt and M. M. Williamson, "Series elastic actuators," in *Proceedings 1995 IEEE/RSJ International Conference on Intelligent Robots and Systems. Human Robot Interaction and Cooperative Robots*, IEEE Comput. Soc. Press, pp. 399–406. doi: 10.1109/IROS.1995.525827.

[207] J. Hollerbach, I. Hunter, and J. Ballantyne, *A comparative analysis of actuator technologies for robotics*. Cambridge, MA, United States: MIT Press, 1992.

[208] G. Zeng and A. Hemami, "An overview of robot force control," *Robotica*, vol. 15, no. 5, pp. 473–482, Sep. 1997, doi: 10.1017/S026357479700057X.

[209] H. Asada and K. Youcef-Toumi, "Design for Joint Torque Sensors and Torque Feedback Control for Direct-Drive Arms," in *Direct-Drive Robots*, The MIT Press, 1987. doi: 10.7551/mitpress/2438.003.0016.

[210] M. Sharifi, V. Azimi, V. K. Mushahwar, and M. Tavakoli, "Impedance Learning-Based Adaptive Control for Human–Robot Interaction," *IEEE Transactions on Control Systems Technology*, vol. 30, no. 4, pp. 1345–1358, Jul. 2022, doi: 10.1109/TCST.2021.3107483.

[211] P. N. Parmar, F. C. Huang, and J. L. Patton, "Evidence of multiple coordinate representations during generalization of motor learning," *Exp Brain Res*, vol. 233, no. 1, pp. 1–13, Jan. 2015, doi: 10.1007/s00221-014-4034-6.

[212] J. S. Sulzer, M. A. Peshkin, and J. L. Patton, "Design of a Mobile, Inexpensive Device for Upper Extremity Rehabilitation at Home," in *2007 IEEE 10th International Conference on Rehabilitation Robotics*, IEEE, Jun. 2007, pp. 933–937. doi: 10.1109/ICORR.2007.4428535.

[213] N. Hogan and S. Buerger, "Impedance and Interaction Control," in *Robotics and Automation Handbook*, 1st ed., T. Kurfess, Ed., CRC Press, 2005.

[214] E. Matheson, R. Minto, E. G. G. Zampieri, M. Faccio, and G. Rosati, "Human–Robot Collaboration in Manufacturing Applications: A Review," *Robotics*, vol. 8, no. 4, p. 100, Dec. 2019, doi: 10.3390/robotics8040100.

[215] A.-N. Sharkawy and P. N. Koustoumpardis, "Human–Robot Interaction: A Review and Analysis on Variable Admittance Control, Safety, and Perspectives," *Machines*, vol. 10, no. 7, p. 591, Jul. 2022, doi: 10.3390/machines10070591.

[216] T. Fujiki and K. Tahara, "Series admittance–impedance controller for more robust and stable extension of force control," *ROBOMECH Journal*, vol. 9, no. 1, p. 23, Dec. 2022, doi: 10.1186/s40648-022-00237-5.

[217] C. Jiang, F. Wang, L. Zhao, H. Wu, and K. Shi, "Admittance Control of Lower Limb Exoskeleton Robot," in *2019 IEEE 9th Annual International Conference on CYBER Technology in Automation, Control, and Intelligent Systems (CYBER)*, IEEE, Jul. 2019, pp. 1131–1135. doi: 10.1109/CYBER46603.2019.9066695.

[218] Shuxiang Guo, Songyuan Zhang, Zhibin Song, and Muye Pang, "Development of a human upper limb-like robot for master-slave rehabilitation," in *2013 ICME International Conference on Complex Medical Engineering*, IEEE, May 2013, pp. 693–696. doi: 10.1109/ICCME.2013.6548339.

[219] Q. Ai, C. Zhang, W. Wu, C. Zhang, and W. Meng, "Design and implementation of haptic sensing interface for ankle rehabilitation robotic platform," in *2018 IEEE 15th International*

Conference on Networking, Sensing and Control (ICNSC), IEEE, Mar. 2018, pp. 1–6. doi: 10.1109/ICNSC.2018.8361366.

[220] S. Liu and J. E. Bobrow, "An Analysis of a Pneumatic Servo System and Its Application to a Computer-Controlled Robot," *J Dyn Syst Meas Control*, vol. 110, no. 3, pp. 228–235, Sep. 1988, doi: 10.1115/1.3152676.

[221] V. Oguntosin, W. S. Harwin, S. Kawamura, S. J. Nasuto, and Y. Hayashi, "Development of a wearable assistive soft robotic device for elbow rehabilitation," in *2015 IEEE International Conference on Rehabilitation Robotics (ICORR)*, IEEE, Aug. 2015, pp. 747–752. doi: 10.1109/ICORR.2015.7281291.

[222] B. A. Valdés and H. F. M. Van der Loos, "Biofeedback vs. game scores for reducing trunk compensation after stroke: a randomized crossover trial," *Top Stroke Rehabil*, vol. 25, no. 2, pp. 96–113, Feb. 2018, doi: 10.1080/10749357.2017.1394633.

[223] K. Shi *et al.*, "Multimodal Human-Exoskeleton Interface for Lower Limb Movement Prediction Through a Dense Co-Attention Symmetric Mechanism," *Front Neurosci*, vol. 16, Apr. 2022, doi: 10.3389/fnins.2022.796290.

[224] L. Shao *et al.*, "EEG-Controlled Wall-Crawling Cleaning Robot Using SSVEP-Based Brain-Computer Interface," *J Healthc Eng*, vol. 2020, pp. 1–11, Jan. 2020, doi: 10.1155/2020/6968713.

[225] S. Vita and A. Mennitto, "NEUROBOT: A psycho-edutainment tool to perform neurofeedback training in children with ADHD," in *CEUR Workshop Proceedings*, 2019.

[226] R. Sorbello *et al.*, "Embodied responses to musical experience detected by human bio-feedback brain features in a Geminoid augmented architecture," *Biologically Inspired Cognitive Architectures*, vol. 23, pp. 19–26, Jan. 2018, doi: 10.1016/j.bica.2018.01.001.

[227] D. Yeung, I. M. Guerra, I. Barner-Rasmussen, E. Siponen, D. Farina, and I. Vujaklija, "Co-Adaptive Control of Bionic Limbs via Unsupervised Adaptation of Muscle Synergies," *IEEE Trans Biomed Eng*, vol. 69, no. 8, pp. 2581–2592, Aug. 2022, doi: 10.1109/TBME.2022.3150665.

[228] C. Li, P. Zheng, S. Li, Y. Pang, and C. K. M. Lee, "AR-assisted digital twin-enabled robot collaborative manufacturing system with human-in-the-loop," *Robot Comput Integr Manuf*, vol. 76, p. 102321, Aug. 2022, doi: 10.1016/j.rcim.2022.102321.

[229] B. A. Valdés and H. F. M. Van der Loos, "Biofeedback vs. game scores for reducing trunk compensation after stroke: a randomized crossover trial," *Top Stroke Rehabil*, vol. 25, no. 2, pp. 96–113, Feb. 2018, doi: 10.1080/10749357.2017.1394633.

[230] J. Kallberg, V. Beitelman, V. Mitsuoka, J. Pittman, M. W. Boyce, and T. W. Arnold, "The Tactical Considerations of Augmented and Mixed Reality Implementation," *Mil Rev*, 2022.

[231] W. J. Tharion, M. J. Buller, A. W. Potter, A. J. Karis, V. Goetz, and R. W. Hoyt, "Acceptability and Usability of an Ambulatory Health Monitoring System for Use by Military Personnel," *IIE Trans Occup*, vol. 1, no. 4, pp. 203–214, Oct. 2013, doi: 10.1080/21577323.2013.838195.

[232] C. Armour and J. Ross, "The Health and Well-Being of Military Drone Operators and Intelligence Analysts: A Systematic Review," *Military Psychology*, vol. 29, no. 2, pp. 83–98, Feb. 2017, doi: 10.1037/mil0000149.

[233] D. Voth, "A new generation of military robots," *IEEE Intell Syst*, vol. 19, no. 4, pp. 2–3, Jul. 2004, doi: 10.1109/MIS.2004.30.